

SunQM-6s2: A Unified Description Of 1D-Wave, 1D-Wave Packet, 3D-Wave, 3D-Wave Packet, and $|n/m\rangle$ Elliptical Orbital Transition for A Photon's Emission and Propagation Using $\{N,n\}$ QM

Yi Cao

e-mail: yicaojob@yahoo.com. ORCID: 0000-0002-4425-039X

© All rights reserved. Submitted to viXra.org on 8/8/2022.

Abstract

Based on paper SunQM-6s1, I re-designed the description for an H-atom's electron movement, the orbital transition, and a photon's emission and propagation. We first used the " $|n/m\rangle$ elliptical orbital model" to replace the Born probability, then used the " $|nL0\rangle$ elliptical orbital transition model" to explain all transition and emission related processes. Therefore, instead of using the electron cloud description, we moved back to the semi-classical physics' orbital description (by using a group of elliptical orbital tracks). We narrowed the (general) QM probability description (i.e., the Copenhagen interpretation) down to the high uncertainty of the momentum vector Δp at the perihelion region of the elliptical orbital track, so that an orbital moving electron can switch (within the same $|n/m\rangle$ QM state), or even transit (between different n of $|n/m\rangle$) between the different elliptical orbital tracks at the perihelion region. We hypothesized that during the orbital transition, the orbital electron spins-off its outmost shell of its 3D wave packet to form a photon. We hypothesized that it is the uncertainty principle $\Delta p \Delta x$ (that equivalent to a QM-force) that first symmetrized the 3D wave packet of a photon (from an un-symmetric newborn photon), and then further trimmed the over-grown 3D wave packet of an old photon (by splitting-out the outmost shell to form a new low-f photon). Then we re-calculated that (to satisfy Hubble constant ~ 70 (km/s)/Mpc), a 656.1 nm photon, after propagating each $\sim 2.7E+10$ meters (about a half distance from Sun to Mercury), it will split-out a 0.02 Hz low-f photon. We emphasized that it is the natural attribute of an old photon to "decay" by red-shifting. Thus, we may have an alternative explanation (other than the "expanding Universe") for the cosmic red-shift. (Note: this is only a citizen scientist-leveled guess). We mathematically built up a 1D-wave packet for a photon, and correlated its emission to the electron orbital movement. We also (qualitatively) described a photon's 3D wave and 3D wave packet. Thus, we (conceptually) unified all four different kinds of wave explanations (1D-wave, 1D-wavepacket, 3D-wave, and 3D wave packet) for a photon's emission and propagation, and also correlated it to the electron's orbital movement in H-atom. This model revealed that a 3D wave packet should have the size about one wavelength.

Key Words: Quantum mechanics, $\{N,n\}$ QM, $|n/m\rangle$ elliptical orbit, photon emission and propagation, 1D wave packet, 3D wave packet, hydrogen atom, uncertainty principle.

Introduction

In memory of Werner Heisenberg (who proposed the uncertainty principle in 1927).

The SunQM study have demonstrated that not only the formation of Solar system ^{[1]~[16]}, but also the formation of the whole universe ^{[17]~[25]}, was governed by its $\{N,n\}$ QM, and the non-Born probability (NBP) can be used to describe

many macro- and micro-world's phenomena ^{[17]~[19], [24]}. The success of the SunQM study makes us to believe that “*all mass entities (from the whole universe to a single quark) can be described by Schrodinger equation and solution*” (see SunQM-3s11 section IX). Then we extend this idea to the force field, re-classified the four fundamental forces into three pairs: G/RFG-force, E/RFE-force and S/RFS-force, and proposed a new $\{N,n\}$ QM field theory (i.e., all force fields can also be described by Schrodinger equation and solution ^[23]). In SunQM-7, we said that we need to expand the Schrodinger equation-based (NBP trajectory) description from the circular orbit to elliptical/parabolic/hyperbolic orbits. In the current paper, we used the newly designed “ $|n/m\rangle$ elliptical orbit” to describe the orbital electron movement in H-atom, and used the “ $|nL0\rangle$ elliptical orbital transition model” to describe a photon's emission and propagation process.

Note: for $\{N,n\}$ QM nomenclature as well as the general notes for $\{N,n\}$ QM model, please see SunQM-1 sections VII & VIII. Note: Microsoft Excel's number format is often used in this paper, for example: $x^2 = x^2$, $3.4E+12 = 3.4 \times 10^{12}$, $5.6E-9 = 5.6 \times 10^{-9}$. Note: The reading sequence for SunQM series papers is: SunQM-1, 1s1, 1s2, 1s3, 2, 3, 3s1, 3s2, 3s6, 3s7, 3s8, 3s3, 3s9, 3s4, 3s10, 3s11, 4, 4s1, 4s2, 5, 5s1, 5s2, 7, 6 and 6s1. Note: for all SunQM series papers, reader should check “SunQM-9s1: Updates and Q/A for SunQM series papers” for the most recent updates and corrections. Note: $|n/m\rangle$ means $|n,l,m\rangle$ QM state, “nLL” or $|nLL\rangle$ means $|n,l,m\rangle$ QM state with $l = n-1 = L$, and $m = n-1 = L$. “nL0” or $|nL0\rangle$ means $|n,l,m\rangle$ QM state with $l = n-1 = L$, and $m = 0$. Note: RF means “RotaFusion”, or “rotation diffusion”. Note: in SunQM-7, the current paper was cited as “SunQM-6s2: Using Bohr atom, $\{N,n\}$ QM field theory, and non-Born probability to describe a photon's emission and propagation (part 2)”.

I. Using the (semi-classical and semi-QM) electron orbital theory to explain electron's motion in H-atom

Even though I am working as a $\{N,n\}$ QM scientist, but most time my thinking is still based on the classical physics. It is worthwhile to re-explain electron cloud and photon emission by using the semi-classical and semi-QM method because it really helps us to understand better.

I-a. The $n=1$ electron cloud in hydrogen atom may should be explained by the classical orbit (or a single electron's uni-directional motion) with precession and RF in different eccentricities and inclinations

(Note: this section was mostly explained in SunQM-7's section-II-b. It is re-explained here (with some major modifications) for the integrated explanation of the whole concept in both section I and section II of current paper). Figure 1a showed a motion electron's Born probability density (only in $\theta\phi$ -2D dimension, or $|Y(0,0)|^2$, in H-atom) in the $n=1$, or $|1,0,0\rangle$ QM state. Here we re-explained the 3D Born probability density as the collection of many single orbital tracks. (Note: Electron orbital tracks like the railway tracks, they are fixed. Here we simplify them as the enclosed circles or ellipses. Electron's motion trajectory likes a train that moving along one of many tracks during one period of time). In Figure 1b, we showed one set of orbit tracks: one circular orbit (with $r_n = r_1$), and many elliptical orbits with different eccentricity (Note: They all have the same semi-major axis that equals to r_1 of the circular orbit, and in the classical elliptical orbital theory, this means all these elliptical and circular orbits have the same orbital energy), and with their major axis on +x axis. (Note: the value of the eccentricity changes continuously, not in discrete, all these tracks are in xz-plane). The electron likes to stay in the dark/thick-line tracks more than in the grey/thin-line tracks. Figure 1c showed that there are many this kind of orbital track sets, each pointing to the different direction to fill all 4π solid angle (just like a single point charge's countless electric force lines filled all 4π solid angle). Notice that Figure 1c only used x' -axis and x'' -axis to represent the countless orbital track sets, each pointing to the different direction to fill all 4π solid angle. After we rotate the orbital track sets about the x' axis (in both + and - directions, so they form prolate spheroid), and then use many of them to fill all 4π solid angle, the collected orbit tracks are equivalent to the Born probability density (as shown in Figure 1d).

We hypothesized that the electron (in H-atom) can only pick one track to do orbit movement at one time. It can switch to its neighboring track at the “most uncertain position” (see more detailed explanation in Figure 3). After the electron went through many (e.g., 10^{10} , notice that this is a randomly guessed number) orbital periods, the collected trajectory also becomes the Born probability density (as shown in Figure 1d). Here we named this hypothesis as the “**electron orbital track model**”. I prefer the “electron orbital track model” (it contains more classical physics description component, even it still contains the orbital Δp uncertainty, see the next two sections) more than the “electron cloud” description (it is purely quantum probability under the Copenhagen interpretation), because I believe that whenever we can use the classical physics to explain, we should use it.

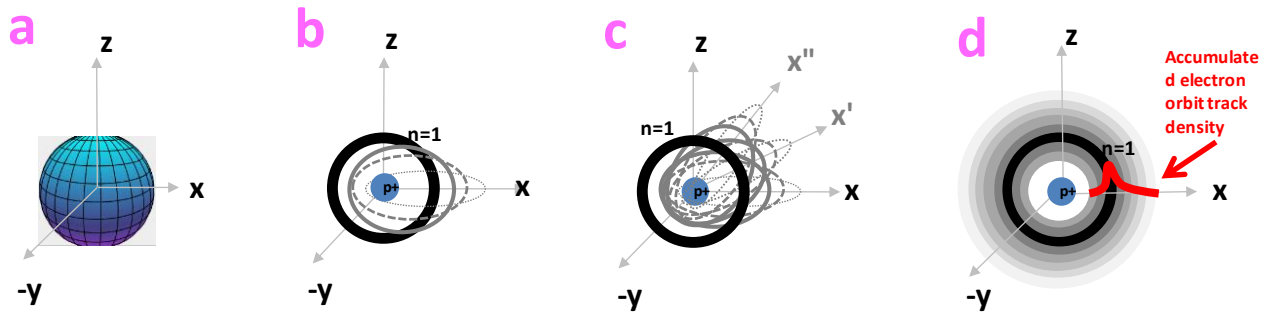


Figure 1a. Plot of $|Y(0,0)|^2$ by using MathStudio (<http://mathstud.io/>) software.

Figure 1(b, c, d). To illustrate that in $\{N,n\}$ QM, how a single orbital track (in H-atom, at $n=1$ QM state) can have many different eccentricities (in Figure 1b), and many orbital tracks (of $n=1$) with all kinds of eccentricities, inclinations, and precessions (in Figure 1c) can be averaged and represented statistically as the Born probability at $n=1$ (in Figure 1d).

Note-1: The elliptical orbits are drawn following the following rule: a) A fixed n quantum number has a fixed length of semi-major axis thus a fixed orbit energy, although it may have many eccentricities; b) In comparison to a low eccentricity orbit, the high eccentricity orbit has its aphelion more outside, so it may have a higher (l quantum number) orbital energy. (Is this the same as Sommerfeld’s theory? I don’t know, although I guess not. If yes, readers please tell me).

Note-2: in Figure 1d, the r -dimensional probability density distribution is a smooth curve (as shown in the red curve along x -axis), and it is not a quantumly changing curve. Sorry as a citizen scientist, I don’t have any plotting software to plot a continuous density change in r -dimension.

I-b. The $n > 1$ electron cloud in Schrodinger QM (and in Bohr hydrogen atom model) may also should be explained by the classical elliptical orbit (or a single electron’s motion) with precession and RF in different eccentricities and inclinations

It is much more difficult to explain a $n > 1$ electron cloud as a collection of a single trajectory of many possible orbital tracks, because it is much less intuitive. Figure 2 (a, b, and c) showed the H-atom’s electron clouds as the Born probability in $|3,2,0\rangle$, $|3,2,1\rangle$, and $|3,2,2\rangle$ QM states (plotted only in $\theta\phi$ -2D). Figure 2 (d, e, and f) showed an attempt to explain the $|3,2,0\rangle$, $|3,2,1\rangle$, and $|3,2,2\rangle$ electron clouds as a set of elliptical orbital tracks. In Figure 2 (c, f) it is obvious that the circular-shaped Born probability density in (and nearly-in) xy -plane is directly caused by the electron’s circular (or near-circular) orbital tracks in (or nearly-in) xy -plane. Then, how to explain Figure 2a’s, or $|3,2,0\rangle$ QM state’s Born probability density as the electron orbital tracks? We explained it as two sets of elliptical orbital tracks. The first set (see Figure 2a’s blue solid-line ellipses, all in xz -plane) of elliptical orbital tracks has its 1st focus point always at the origin of xyz -coordinate, and the aphelion is on the $+z$ axis, with different eccentricities. Notice that the thick lines (in blue) always represent a large amount of (collectively averaged) tracks that the electron likes to stay (or the high probability orbit, or roughly to say, an

averaged orbit in that QM state), while the thin lines (in blue) always represent a few of collective trajectories that electron rarely to stay (or the low probability orbit). Also notice that the aphelion sometimes may move away from the +z axis (or, the major axis of the ellipse may tilt/wobble a little bit (up to around 15 degrees?), let's name the tilted z-axis as z'-axis). When we rotate all these elliptical orbital tracks first about its major axis (i.e., the wobbling z'-axis), and then further rotate about z-axis, it forms a prolate spheroid (like an American football) probability density as shown in Figure 2a (the up part). Then, a second set (see Figure 2d's black dash-line ellipses) of elliptical orbits is almost exactly the same as of that the first set, except that its second focus is on (or near) the -z axis.

For $|3,2,1\rangle$ QM state's Born probability density, its explanation (as the electron orbital tracks) is pretty much the same as that for $|3,2,0\rangle$. The major difference is, the major axis of the set of blue solid-line elliptical orbits (in xz-plane) now aligns to z'-axis, and z'-axis is tilted away from z-axis by 45 degree. Furthermore, this z'-axis is also wobbling around the $45^\circ \pm 15^\circ$ range. Then, you rotate all these elliptical orbital tracks first about its major axis (i.e., the wobbling z'-axis), and then further rotate about z-axis, it forms a probability shape as shown in Figure 2b (the up part).

Here is a question: why we use Born probability (rather than directly using non-Born probability, NBP) in Figure 2 (or even in Figure 1)? Let's use $|3,2,1\rangle$ QM state, or Figure 2b and Figure 2e as the example for the explanation. The answer is: we simply don't know what the NBP density shape of $|3,2,1\rangle$ should look like, but we do know what the Born probability density shape of $|3,2,1\rangle$ should look like (i.e., the Figure 2b). So, to figure out how a $|3,2,1\rangle$ QM state electron's orbit, we have to start from the $|3,2,1\rangle$ QM state's electron density map (i.e., the Born probability density map). In SunQM-4s1, we have showed that Born probability is the standing wave of two opposite propagational NBP matter wave. Therefore, we said that each single orbital track in Figure 2e describes both two opposite directional orbital movement (in same probability), and the first rotation about z'-axis containing two opposite directional rotations, and the second rotation about z-axis also containing two opposite directional rotations. All these two opposite orbital movement and two opposite directional rotations are always in equal amount and in equilibrium. Thus, the whole collection of orbital tracks shown in Figure 2e becomes the Born probability shown in Figure 2b. Then, for the NBP description, we believe that on each orbital track, we only need to change the bi-directional motion into unidirectional motion, the orbital tracks are still the same.

Next question: why we don't use $r\theta\phi$ -3D Born probability density map, only use $\theta\phi$ -2D Born probability here? The answer is also simple, we don't have the plotting software, or at least I (as a citizen QM scientist) don't have (or can't afford) the plotting software (see SunQM-6s1's Appendix).

Notice that (under some special cases) the whole set of $|3,l,m\rangle$ orbits can also be re-described as $|1,0,0\rangle$ orbit. See Appendix A for more discussion.

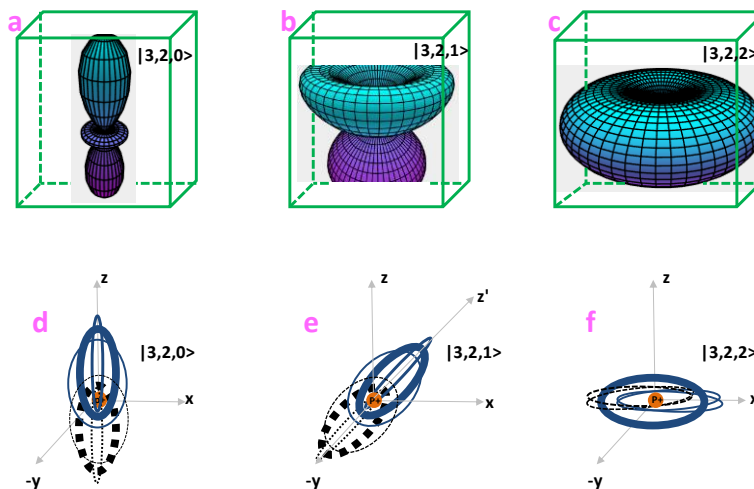


Figure 2 (a, b, and c): Plots of $|Y(2,0)|^2$, $|Y(2,1)|^2$, and $|Y(2,2)|^2$ by using MathStudio (<http://mathstud.io/>) software. Note: the size and orientation of each plot is readjusted by the author due to the technical limitation. (Also see John S. Townsend, A Modern Approach to Quantum Mechanics, 2nd ed., 2012. Page 335, Figure 9.11).

Figure 2d. Illustration of how to use a group of elliptical orbits to replace the electron cloud at $|3,2,0\rangle$ QM state. Note: All ellipses are in xz -plane.

Figure 2e. Illustration of how to use a group of elliptical orbits to replace the electron cloud at $|3,2,1\rangle$ QM state. Note: z' -axis is in xz -plane and pointing away from z -axis by 45° . All elliptical orbits are in xz -plane.

Figure 2f. Illustration of how to use a group of elliptical orbits to replace the electron cloud at $|3,2,2\rangle$ QM state. Note: Major orbits (thick dark line) are in xy -plane, minor orbits (thin grey line) tilted out of (and wobbling around) xy -plane.

I-c. The hypothesis that “the most uncertain region” in an elliptical orbital track is at the perihelion site

The $\{N,n/q\}$ QM theory showed us that the rotation diffusion (or RotaFusion, or RF) is a natural attribute of the orbital movement. In other words, for a bound state object (e.g., electron, planet, etc.) that doing orbital movement, it always has RF. For example, an electron (in H-atom), if at $n=1$ QM state, or at any n (i.e., $|n/m\rangle$ with a complete set of $l = 0..n-1$ and $m = -l..+l$) QM state, it will have a complete RF; if at any single nLL (i.e., $|n,l_{(-n-1)},m_{(-n-1)}\rangle$) QM state, it will have less RF (see SunQM-2’s Table 6); the only time the orbital motion $RF \rightarrow 0$ is at a single nLL QM state with $n \rightarrow \infty$. Planet Mercury has large orbital precession (which is RF), and planet Earth also has small orbital precession (or RF). With “first principal thinking”, we believe that the RF has to be originated from the uncertainty principle $\sigma_p \sigma_x \geq \hbar/2$ (which is also one of the natural attributes of QM). Or, RF and the uncertainty principle are the same thing. Here, (as a citizen scientist), I like to use the old expression of uncertainty principal $\Delta p \Delta x \geq \hbar/2$ (because it is easier for me to understand, even it may be not accurate). From the common knowledge of daily life, when driving a car to make a sharp turn at a high speed, it is always harder to control the direction (in comparison to that either the less sharp turn, or the low driving speed). Similarly, based on the Newtonian physics (or the Kepler’s law), for an elliptical orbital movement, we believe that the motion object’s momentum vector direction is less certain, or more uncertain at the perihelion site (where it has the fastest speed and the sharpest turn) than anywhere else. Based on Bohr’s “correspondence principle”, we believe that this is also true for the electron’s (elliptical) orbital movement in H-atom. Figure 3d showed one example (of illustration): a motion electron in an elliptical orbit (in the xz -plane) at the perihelion should have the momentum vector \vec{p} accurately point to the tangential direction (also in xz -plane). However, due to the high speed and sharp turn, the real momentum vector (shown as \vec{p}') may deviate a little bit away from \vec{p} . Notice that \vec{p}' could be also out of xz -plane a little bit, so we believe that the uncertainty vector $\Delta\vec{p} = \vec{p}' - \vec{p}$ is a 3D vector. We further believe that the uncertainty vector $\Delta\vec{p}$ also follows kind of uncertainty principal $\Delta\vec{p} \Delta\vec{x} \geq \hbar/2$ (although I am not able to prove it mathematically). From the common sense, we believe that for a circular orbit movement, the uncertainty vector $\Delta\vec{p}$ is evenly distributed everywhere (see Figure 3a), for an elliptical orbit with low eccentricity, $\Delta\vec{p}$ distributed more at the perihelion (half-circle) side (see Figure 3b), and for an elliptical orbit with high eccentricity, $\Delta\vec{p}$ is highly concentrated at the perihelion position (see Figure 3c). Thus, we define the “**most uncertain position**”, it is at the perihelion region for an elliptical orbit, with the highest $\Delta\vec{p}$ uncertainty vector.

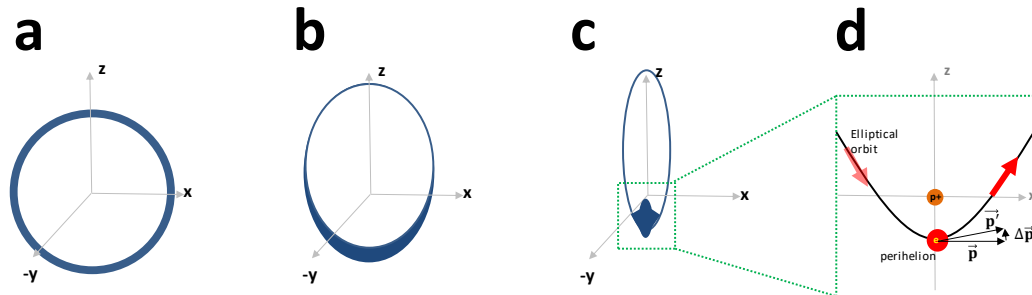


Figure 3 (a, b, c). The (blue) thickness represent the uncertainty of either $\Delta\vec{p}$ (or $\Delta\vec{x}$, in 3D). (Note: it does not represent the probability of the orbital track that electron like to stay). The thicker, the higher uncertainty of $\Delta\vec{p}$ (or $\Delta\vec{x}$, in 3D) for the trajectory of the motion electron.

Figure 3d. To illustrate that an elliptical orbital moving electron has an uncertain $\overline{\Delta\vec{p}} = \vec{p}' - \vec{p}$ that may point to any direction in 3D space.

I-d. How electron switches the orbital track from one to another? It may be driven by the uncertainty force (or the RF-force)

Figure 4 tried to explain that how an orbital moving electron (in $|3,2,0\rangle$ QM state) switch from the one orbital track to another (and both tracks belong to $|3,2,0\rangle$ QM state). In Figure 4a, all ellipses represent the $|3,2,0\rangle$ QM state electrons' orbital tracks (and suppose all of them are in xz-plane). Again, the thick (solid and dashed) lines represent the highly favored tracks, and the thin (solid and dashed) lines represent those disfavored tracks. In Figure 4b, we named an extreme elongated track (the thin solid line) as "track-1", and named a less-elongated track that also tilted a little bit (the thin dashed line) as "track-2". (Notice that both track-1 and track-2 belongs to $|3,2,0\rangle$ QM state). Then, Figure 4b showed that a moving-in electron followed the track-1 (as shown in half-transparent red arrows), and almost suddenly (or quantumly) changed to track-2 at the perihelion site, and then moved out (as shown in the solid red arrows). Figure 4c showed that the motion electron changed the track at the perihelion site where the uncertainty of $\Delta\vec{p}$ is the maximum (represent in the blue vertical bars in perihelion region), so that the real momentum vector \vec{p}' is deviated upward a little bit (still in xz-plane, as shown in Figure 3d), and also the position vector \vec{x}' deviated a little bit. From the classical physics, this kind of $\Delta\vec{p}$ $\Delta\vec{x}$ change will produce an outgoing trajectory with the ellipse titled a little bit (anti-clockwise in xz-plane), and with a smaller eccentricity. Then, considering the real momentum vector $\Delta\vec{p}$ and the position vector $\Delta\vec{x}$ may deviate within any of the possible (3D) solid angle, it will cause the electron to switch to any possible nearby tracks (in and out xz-plane), and causing RF.

Notice that in this model, each $\Delta\vec{p}$ change, or $\Delta\vec{x}$ change, or $\Delta\vec{p}$ $\Delta\vec{x}$ change, is always very small, so that the motion electron can only switch from one track to the very neighboring track. We need to emphasize that the electron movement is based on (the classical physics) $\delta d = v \delta t$, where the velocity v varies upon the position in the elliptical orbit (according to the Kepler Law). There is no "quantum jumps" in this description. Notice that the "quantum jumps" means when $\delta t \rightarrow 0$, $\Delta\vec{x} > 0$; while no "quantum jumps" means when $\delta t \rightarrow 0$, $\Delta\vec{x} \rightarrow 0$. For example, in Figure 3b, a motion electron at the red ball position, after a δt , it can only move to $\delta d = v \delta t$ to the blue ball position, it cannot jump to the orange ball position (because $\delta d > v \delta t$). It also cannot jump to the green ball position (even it fits $\delta d = v \delta t$), because the direction change of \vec{p}' vector is too big for the uncertainty of $\Delta\vec{p}$ (or the kind of $\Delta\vec{p}$ $\Delta\vec{x} \geq \hbar/2$, also see the green circular sector shape in Figure 3c for the illustration of the allowed \vec{p}' vector deviation). In contrast, the electron cloud description seems does allow the (relatively) large scale "quantum jumps" (if I did not understand wrong).

Then, in Figure 3a, how the $n=3$ electron switch from the (upward) extreme elongated solid line $|3,2,0\rangle$ track to the (downward) extreme elongated dash-line $|3,2,0\rangle$ track?

1) For the undisturbed (meaning no outside force field) H-atom, it started from extreme up-elongated $|3,2,0\rangle$ track, gradually switch tracks to the averaged up-elongated $|3,2,0\rangle$ (the grey thick line), then to the averaged up-elongated $|3,1,0\rangle$ tracks, then to the averaged circular $|3,0,0\rangle$ tracks (notice that in the undisturbed H-atom, they all have the same orbital energy because they have the same $n=3$ quantum number, even different with l quantum numbers), then to the averaged down-elongated $|3,1,0\rangle$ tracks, then to the averaged down-elongated $|3,2,0\rangle$ tracks, and finally to the extreme down-elongated $|3,2,0\rangle$. The whole process may take 10^{10} (a randomly guessed number) round of orbital movement to finish.

2) For a H-atom under the outside-force field, beside the above path, there may (or may not) exist a second path: it started from extreme up-elongated $|3,2,0\rangle$ track, gradually switch tracks to the averaged up-elongated $|3,2,1\rangle$, then to the averaged near-circular $|3,2,2\rangle$ tracks, then to the averaged down-elongated $|3,2,1\rangle$, then to the averaged down-elongated $|3,2,0\rangle$, and

finally to the extreme down-elongated $|3,2,0\rangle$. Because all these $|3,2,m\rangle$ orbits have the same n and l , thus have the same orbital energy. The whole process may take 10^{10} (a randomly guessed number) round of orbital movement to finish.

Also notice that the possibility that an electron moves to the extreme elongated $|3,2,0\rangle$ track is extremely low (e.g., 10^{-10} , purely guessed number). We named this model as the “ $|n/m\rangle$ elliptical orbit model”.

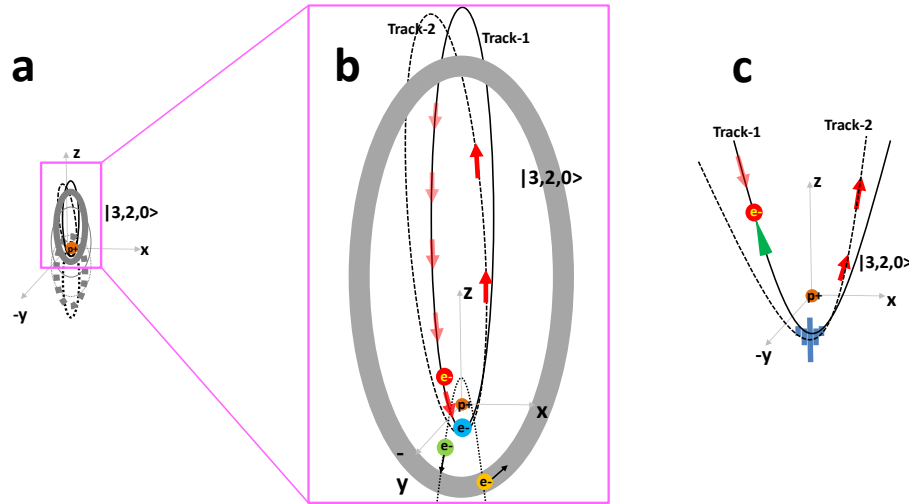


Figure 4. Illustration of RF motion of an electron in the orbit of $|3,2,0\rangle$ QM state. (Note: All ellipses are in xz -plane).

Figure 4a. Illustration of how to use a group of elliptical orbits to replace the electron cloud at $|3,2,0\rangle$ QM state.

Figure 4b. Using the “ $|n/m\rangle$ elliptical orbit model” to illustrate the RF motion of an electron in the $|3,2,0\rangle$ elliptical orbit by switching from track-1 to track-2 (shown in red arrows).

Figure 4c. To illustrate the RF motion of an electron that moves from track-1 to track-2 (shown in red arrows) at the highest uncertainty (shown in blue bars) perihelion region (in $|3,2,0\rangle$ elliptical orbit).

I-e. Summary and discussion (on section I)

1) We repetitively mentioned that in $\{N,n\}$ QM, the uncertainty principle and RF are the same thing, and both of them are often treated as a kind of QM-force;

2) The key point is, the electron cloud is only an auxiliary concept in QM, it describes the averaged electron motion (for $\sim 10^{10}$ round of orbital movement). An orbital electron’s motion should can be described in more detail than the “cloud”. One example we showed in SunQM-7 was: assuming that we collected 100 rounds of Mercury’s precessional orbital movement trajectory, and (if) found it can be described by nLL QM state with $n' = 3 \cdot 6^4 = 3888$, or $|3888,3887,3887\rangle$ QM state, then we collect 100 rounds of an electron (in a H-atom, also at $|3888,3887,3887\rangle$ QM state)’s orbital motion trajectory, we should find the electron’s trajectory is very similar as that of planet Mercury’s trajectory in terms of their inclination, eccentricity, and precession;

3) Here is one question: Does the low eccentric orbit mostly has small, slower (and more continues) precession, while the high eccentric orbit may have (relative) larger (or more quantum) precession?

4) By doing so, we conceptually unified the Schrodinger equation (with Born Prob, and NBP) and elliptical orbit description (see more discussion section III).

II. Using the (semi-classical and semi-QM) electron orbital theory to explain a photon's emission (and absorption) process in H-atom

II-a. Using Bohr atom model's $n=3$ and $n=2$ circular electron orbits to explain a photon's emission process.

See SunQM-6s1's Figure 1, and the explanation.

II-b. The (hypothesized) physical structure of an electron (based on $\{N,n/6\}$ QM structure, i.e., a 3D matter wave packet) with multiple shells and a dis-entangle-able outmost shell

Here we hypothesized that an electron has the physical structure (i.e., a 3D matter wave packet) of multiple shells and a core that based on $\{N,n\}$ QM (like that of photon's, see SunQM-6s1's Figure 4). All these shells are entangled with each other, and with the core. This structure not only explained electron's particle-wave duality property, but also explained electron's double-slit experiment result (see the explanation in SunQM-6s1's section III). We further hypothesized that under the extreme situation (e.g., when a fast-moving electron is forced to make a sharp turn), its outmost shell could be spun-off (or dis-entangled) from its main body, and forming a new low-frequency 3D matter wave energy packet and then emitted as a photon. This is similar to the explanation that during the propagation, an old photon will dis-entangle its outmost shell (to be a low-f photon) and cause the cosmic redshift (see SunQM-6s1's section IV, also see section II-j for some calculations).

II-c. Using $|3,2,0\rangle$ QM state's elliptical orbit to re-explain a photon's emission process in H-atom

In a rare case, the $|3,2,0\rangle$ QM state's extreme elongated elliptical orbital track (in xz -plane, see the black solid-thin line ellipse in Figure 5a) has its perihelion (approximately) overlapping with the perihelion of the $|2,1,0\rangle$ QM state's (the averaged) elliptical orbital track (also in xz -plane, see the blue solid-thick line ellipse in Figure 5a). A motion electron at this position (see Figure 5b's red-ball), due to has the highest uncertainty of \vec{p} in both tracks, can go to either the $|3,2,0\rangle$ extreme elongated (black-thin) track, or the $|2,1,0\rangle$ (the averaged, blue-thick) track, depending on the orbital velocity value of this electron at this position. According to the classical physics (or the Kepler's law), an electron (or a planet) at the perihelion with high orbital velocity will follow a highly-elongated elliptical track, and vice versa. A move-in $|3,2,0\rangle$ electron at the perihelion will keep in the same $|3,2,0\rangle$ track to move out if it keeps the original (high) orbital velocity. However, if it decelerates quantumly (in $+x$ direction) at the perihelion point (by spin-off its outmost shell as a low-frequency energy packet (i.e., a photon) along $+x$ direction, so the emitted photon takes away some momentum from the electron, and this taken-away momentum has zero mass associated with it), then the electron's out-moving trajectory will quantumly transit to a low eccentricity track (e.g., the $|2,1,0\rangle$ track). This electron deceleration by emitting a (656.1 nm) photon process follows the linear momentum conservation at the perihelion point (shown in Figure 5b, red ball). There, the linear momentum of the electron at $n=3$ is $p_{3,p} = m_e v_{3,p}$, at $n=2$ $p_{n,p} = m_e v_{2,p}$, the lost linear momentum is $\Delta p_{3-2} = m_e (v_{3,p} - v_{2,p})$, and this lost linear momentum is passed to the emitted photon $\Delta p_{3-2} = h/\lambda$. Solving the equation, we obtained that the loss of the electron's (linear-directional) velocity at perihelion is $(v_{3,p} - v_{2,p}) = h/\lambda / m_e = 6.6261E-34 \text{ (J*s)} / (656.1E-9 \text{ (meter)}) / 9.1094E-31 \text{ (kg)} \approx 1109 \text{ m/s}$. (Note: for the circular/elliptical orbital motion, the angular momentum (but not the linear momentum) is conserved). From the energy conservation, we obtained that the emitted photon has frequency of $\Delta f_{3 \rightarrow 2,ph} = f_{n=3,ph} - f_{n=2,ph} = 3.66E+14 - 8.22E+14 = 4.57E+14 \text{ (Hz)}$, (see SunQM-6s1's Table 1). Thus, we successfully unified the classical description

and the $\{N,n\}$ QM description for the photon emission (for an H-atom's $n=3$ to $n=2$ transition). We named this description as the “ **$nL0$ elliptical orbital transition model**”.

More discussions (on section II-c):

- 1) Notice that after passing the perihelion point, the main body of the 3D wave packet of electron (i.e., the de-excited electron) moves in near z-direction (from perihelion to aphelion), while the dis-entangled outmost shell of the electron (i.e., the photon) moves in x-direction. This is because the (de-excited) electron is always attracted by the proton, so that its momentum vector is always modulated by the electric force. While the electron's spun-off outmost shell (i.e., the emitted photon, or the energy 3D wave packet, or the momentum 3D wave packet) is neutral of charge, and it is not attracted by the proton's electric force, so the emitted photon propagates is at the tangential direction (i.e., the x-direction) of the perihelion point (of the elliptical orbit) where it initially separated from its mother body (i.e., the $n=3$ electron).
- 2) For the $n=3$ to $n=2$ transition, (we guessed that) the $n=3$ electron first orbits in the averaged $|3,2,0\rangle$ elliptical track for many rounds, and then occasionally goes to the extreme elongated $|3,2,0\rangle$ elliptical track, and then transits to the extreme elongated $|2,1,0\rangle$ elliptical track at the overlapped perihelion site (at a very low probability). Then, the electron gradually relaxes to the averaged $|2,1,0\rangle$ elliptical track after many rounds of orbital movement. (Note: in the real case, the RF movement that out of xz-plane need also be added in the description. Also see one real calculation by using this model in section II-d).
- 3) As for SunQM-6s1's Figure 1a, we can describe both circular orbits in xy-plane as in $|3,2,2\rangle$ and in $|2,1,1\rangle$ QM states, and the emitted photon is also in +x direction. This is consistent with the Figure 5 (in this paper) that both the $n=3$ orbit (at $|3,2,0\rangle$ QM state) and the $n=2$ orbit (at $|2,1,0\rangle$ QM state) are at xz-plane, and the emitted photon is in +x direction. Although $|3,2,0\rangle$ elliptical orbit has its own transient orbital frequency at each position on the track, the (weighted) averaged frequency over the whole period of elliptical orbit of $|3,2,0\rangle$ should equal to the $|3,2,2\rangle$ circular orbit's frequency $f_{3,ph}=3.66E+14$ Hz. This should also be true for $|2,1,0\rangle$ and $|2,1,1\rangle$ orbits.

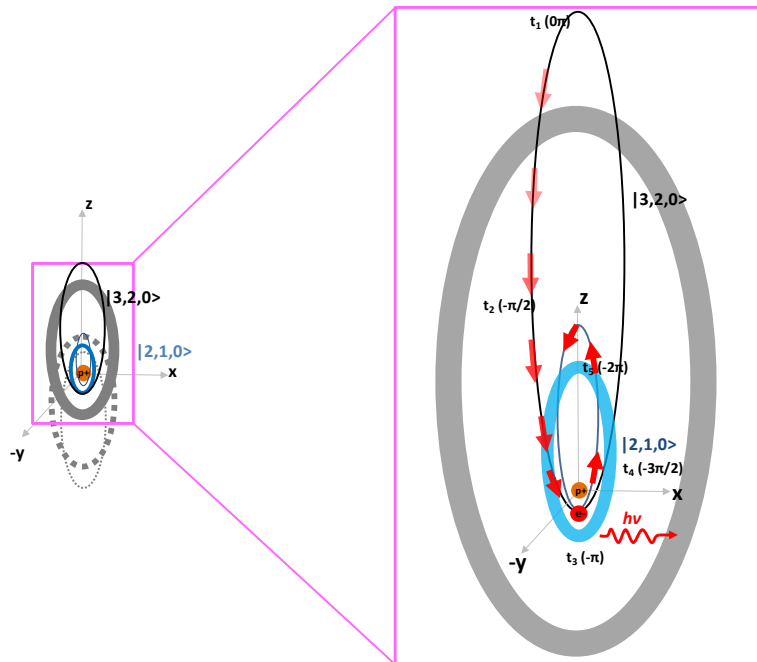


Figure 5a (left). Illustration of how to use a group of elliptical orbits to replace the Born probability at $|3,2,0\rangle$ and $|2,1,0\rangle$ QM state. (Note: All ellipses are in xz-plane).

Figure 5b (right). Illustration of the trajectory of electron transit from $|3,2,0\rangle$ to $|2,1,0\rangle$ elliptical orbits (both are in xz-plane), and the photon emission (in +x direction). The thick-line ellipses in grey and blue represent the averaged tracks of $|3,2,0\rangle$ orbits and $|2,1,0\rangle$ orbits. The thin-lined ellipses in black and blue represent the extreme elongated (low probability) orbit of $|3,2,0\rangle$ and $|2,1,0\rangle$. According to one model (see section II-d), two perihelion sites (of these two extreme elongated elliptical

orbits) overlap at the near the surface of the proton. In an alternative model (see section II-e), we can use the less extremely elongated elliptical orbits for $|3,2,0\rangle$ and $|2,1,0\rangle$, so that the two perihelion sites are not overlap one to another, and the both perihelion points are (comfortably) not too close to the H-atom's nucleus (i.e., the proton).

II-d. Can we calculate out two real orbits for the $|3,2,0\rangle$ to $|2,1,0\rangle$ elliptical orbital transition?

In this section, we tried to calculate out a “real” elliptical orbit track (here “real” means mathematically solvable, not necessary physically real) for a H-atom's $|3,2,0\rangle$ to $|2,1,0\rangle$ transition (with the condition that at the perihelion site, $\Delta\vec{p} > 0$ and $\Delta\vec{x} = 0$). First, we used the classical physics method to calculate. In SunQM-6s1's Table 1, we calculated the Bohr H-atom's orbital energy $E_3 = -2.421\text{E-}19$ (Joule), $E_2 = -5.447\text{E-}19$ (Joule). According to wiki "Elliptic orbit", “For a given semi-major axis the specific orbital energy is independent of the eccentricity”. So, as long as $|3,2,0\rangle$ elliptical orbital track has the semi-major axis equals to Bohr atom's $r_{n=3}$, we assumed that they have the same $E_{n=3}$. Thus, we have the $|3,2,0\rangle$ elliptical orbital track's energy at the perihelion position $E_{3,p}$:

$$E_{3,p} = K + U = \frac{1}{2}mv_{n=3,p}^2 - \frac{Ze^2}{4\pi\epsilon_0 r_{n=3,p}} = -2.421 \times 10^{-19} \text{ (Joule)} \quad \text{eq-1}$$

where $v_{n=3,p}$ is the electron's orbital transient velocity at perihelion, and $r_{n=3,p}$ is the orbital moving electron's transient radius at perihelion. Similarly, we have

$$E_{2,p} = K + U = \frac{1}{2}mv_{n=2,p}^2 - \frac{Ze^2}{4\pi\epsilon_0 r_{n=2,p}} = -5.447 \times 10^{-19} \text{ (Joule)} \quad \text{eq-2}$$

In our hypothesis, the photon emission happened at

$$r_{n=3,p} = r_{n=2,p} \quad \text{eq-3}$$

From the (linear) momentum conservation (of the electron at the perihelion position), we have

$$m_e v_{n=3,p} = m_e v_{n=2,p} + \frac{h}{\lambda} \quad \text{eq-4}$$

where $\lambda = 656.1$ nm. Solving this jointed four equations for four unknowns ($v_{n=3,p}$, $r_{n=3,p}$, $v_{n=2,p}$, and $r_{n=2,p}$), we obtained:

$$v_{n=3,p} \approx 2.99550594\text{E}+8 \text{ m/s}, \quad \text{eq-5}$$

$$v_{n=2,p} \approx 2.99549485\text{E}+8 \text{ m/s}, \quad \text{eq-6}$$

(notice that $v_{n=2,p} < v_{n=3,p} < c = 2.99790000\text{E}+8$ m/s, the light speed),

$$v_{n=3,p} - v_{n=2,p} \approx 1109 \text{ m/s}, \quad \text{eq-7}$$

(thus, the elliptical orbital moving electron could be treated as quantumly decelerated at the perihelion), and

$$r_{n=3,p} = r_{n=2,p} \approx 5.645\text{E-}15 \text{ meters}. \quad \text{eq-8}$$

(Notice that it is larger than the proton radius $8.4\text{E-}16$ meters, see SunQM-1s2's Table 1. It means that the moving electron's perihelion radius is still at the outside of H-atom's nucleus, even it is very close to the nucleus). Furthermore, we obtained that the $|3,2,0\rangle$ elliptical orbital track has the extreme high eccentricity

$$e_{|3,2,0\rangle,p} = (a_{n=3} - r_{n=3,p}) / a_{n=3} = (4.763\text{E-}10 - 5.645\text{E-}15) / (4.763\text{E-}10) = 0.999988, \quad \text{eq-9}$$

where $a_{n=3}$ is the semi-major axis of $|3,2,0\rangle$ that equals to the Bohr atom's $r_{n=3} = 4.763\text{E-}10$ meters. (Notice that this extremely high eccentricity means this track has extremely low probability for an orbital moving electron to stay. It also means that the uncertainty of Δp is concentrated sharply at the perihelion site, see Figure 3c. From the sense of the general physics, the extreme high speed and extreme sharp turn at the perihelion must produce an extreme high tendency for an

orbital moving electron to spin-off the “out-coat” from it). Also, the $|2,1,0\rangle$ elliptical orbital track has the extreme high eccentricity

$$e_{|2,1,0\rangle, p} = (a_{n=2} - r_{n=2,p}) / a_{n=2} = (2.117E-10 - 5.645E-15) / (2.117E-10) = 0.999973. \quad \text{eq-10}$$

where $a_{n=2}$ is the semi-major axis of $|2,1,0\rangle$ that equals to the Bohr atom’s $r_{n=2} = 2.117E-10$ meters. (Note: this calculation is based on $\Delta\vec{x} = 0$, so even the math looks fine, the real physical trajectory of the elliptical orbital moving electron will not follow this extreme parameter, see section II-e for the reason).

But, when we tried to apply the same (classical physics) method to the element with high Z-number, it did not work. For example, the X-ray (K_α line, see Giancoli’s book, p1055, Example 39-6) of Mo ($Z=42$) from $n=2$ to $n=1$ transition, the resulted $v_{n=2,p} \approx 3.01124495E+8$ m/s was greater than the speed of light, and the resulted $r_{n=2,p} \approx 5.466E-15$ meters was inside the nucleus of Mo ($r_{\text{nuclear}} = 5.72E-15$ meters, see SunQM-5’s Table 2, column 8). We believed this bad result came from that we had forced $\Delta\vec{x} = 0$ (see section II-e for the reason), rather than the elliptical orbital track model was wrong.

In one calculation, when we tried to use the relativistic method (based on Kraft’s method ^[26]) for the Bohr H-atom, it did not work. The resulted $r_{3,p,\text{relativistic}} \approx 7.30E-18$ meters is inside the nucleus of H-atom ($r_{\text{proton}} = 8.40E-16$ meters). We also believe this bad result came from that we had forced $\Delta\vec{x} = 0$.

II-e. A more accurate method (by including the Δx uncertainty in r-direction) is needed for this model

At the perihelion site, besides the transient momentum uncertainty (Δp), in theory, there should also exist a transient position uncertainty (Δx). In the current section, we tried to do a calculation with both the transient momentum uncertainty $\Delta p > 0$, and the transient position uncertainty $\Delta x > 0$. Using the same example of H-atom’s $n=3$ to $n=2$ transition, it means that at the perihelion site, the transient $r_{n=3,p}$ may be longer than the transient $r_{n=2,p}$ by Δx , and the transient Δx value is determined by the uncertain principle of $\Delta p \Delta x = \text{constant}$ (Sorry, this is a citizen scientist’s expression). Even more, we believed that the $\Delta p \Delta x$ is a transient value in the elliptical orbital movement (e.g., the $\Delta p \Delta x$ transient value at the perihelion site may be larger than that at the aphelion site). As a citizen scientist, I don’t have the ability to deduce out the exact mathematical formula for this thought. Thus, we only tried a very simple test: for the orbital transition from $|3,2,0\rangle$ elliptical orbit’s perihelion site to $|2,1,0\rangle$ elliptical orbit’s perihelion site, assuming there is a fixed a $\Delta p = 1109$ m/s quantum deceleration only in θ -1D dimension (in xz -plane), also assuming there is a fixed a Δx quantum positional jump only in r -1D dimension (in xz -plane). Now in Table 1, we searched several possible values for Δx that satisfy the eq-1 through eq-4 (notice that eq-3 now become $r_{n=3,p} = r_{n=2,p} + \Delta x$). My favorite result (see the yellow row in Table 1) was: if we allowed the electron to (quantum) jump inward by $\Delta r = \Delta x = 1.0E-12$ meters at the perihelion site (the same time when the orbital speed decreased by 1109 m/s in θ -direction) when transiting from $|3,2,0\rangle$ to $|2,1,0\rangle$, then we would obtain a $|3,2,0\rangle$ elliptical orbit with eccentricity $e = 0.94$, $r_{3,p} = 2.83E-11$ meters, $v_{3,p} = 4.17E+6$ m/s, and the ratio of Δx over $r_{3,\text{circular}} = 0.21\%$.

More discussions (on section II-e):

- 1) To me, this result seems physically more possible than what we obtained in section II-d, (because there, $r_{3,p}$ and $r_{2,p}$ are too close to the surface of proton, and $v_{3,p}$ and $v_{2,p}$ are too close to the speed of light, to be physically possible). Also, with both the $v_{3,p}$ and $v_{2,p}$ ($\approx 4.17E+6$ m/s) much slower than the light speed, we don’t have to use the relativistic calculation.
- 2) On the other hand, section II-d gave a single result (from the calculation), while Table 1 only give us many possible results, because $\Delta r = \Delta x$ may be any one value in the table.
- 3) In Table 1, the vector production $\Delta\vec{p} \Delta\vec{x} = 0$, because they are in perpendicular directions. However, in general, the $\Delta\vec{p}$ vector change should be in $r\theta\phi$ -3D dimension (rather than θ -1D only), and $\Delta\vec{x}$ vector change should also be in $r\theta\phi$ -3D dimension (rather than r -1D only), so that it may should follow the 3D vector $\Delta\vec{p} \Delta\vec{x} \geq \hbar/2$ kind of relationship. (Note: A more correct form may be the Gaussian distribution of the 3D vector $\sigma_{\vec{p}} \sigma_{\vec{x}} \geq \hbar/2$. But that is beyond what I can do).
- 4) So, quantitatively, it is not easy to get an accurate result from this model. However, qualitatively, we still can use this over simplified model (i.e., assuming $\Delta\vec{x} = 0$, only allow $\Delta\vec{p}$ change quantumly) to explain the orbital transition.

5) In section II-i, after more discussion on the uncertainty principle, we will learn that the changes of $\Delta\vec{p}$ and $\Delta\vec{x}$ are spread over the whole one period of elliptical orbit (started from aphelion, maximum at perihelion, then ended at aphelion), not only at the perihelion point. Then, the whole $\Delta\vec{p} \Delta\vec{x} \geq \hbar/2$ will make more sense.

6) In Figure 5, if $\Delta r = \Delta x = 0$, then the perihelion positions of both the $|3,2,0\rangle$ and the $|2,1,0\rangle$ elliptical orbits should be drawn in overlap. If allowing $\Delta r = \Delta x > 0$, the $r_{3,p}$ should be drawn larger than $r_{2,p}$.

Table 1. Searching the possible Δx values (under $\Delta p=1109$ m/s) for the elliptical orbital transition at the perihelion site between $|3,2,0\rangle$ and $|2,1,0\rangle$ elliptical orbits.

	$\Delta x = \Delta r$ $= r_{3,p} - r_{2,p}$	$r_{2,p} =$	$v_{2,p} =$	$r_{3,p} = r_{3,p} +$ Δx	$v_{3,p} = v_{2,p} +$ 1109	$\Delta x/r_{3,cir}$	eccentricity (n=2)	eccentricity (n=3)
	m	m	m/s	m	m/s	m/m	m/m	m/m
	1.00E-18	3.56E-14	1.19E+07	3.56E-14	1.19E+07	0.0000002%	0.999832	0.999925
	1.00E-17	1.00E-13	7.12E+07	1.00E-13	7.12E+07	0.0000021%	0.999528	0.999790
	1.00E-16	2.97E-13	4.13E+07	2.97E-13	4.13E+07	0.000021%	0.998599	0.999376
elliptical orbit	1.00E-15	9.09E-13	2.36E+07	9.10E-13	2.36E+07	0.00021%	0.995712	0.998088
	1.00E-14	2.82E-12	1.34E+07	2.83E-12	1.34E+07	0.0021%	0.986698	0.994055
	1.00E-13	8.79E-12	7.51E+06	8.89E-12	7.51E+06	0.021%	0.96	0.98
	1.00E-12	2.73E-11	4.17E+06	2.83E-11	4.17E+06	0.21%	0.87	0.94
	1.00E-11	8.28E-11	2.22E+06	9.28E-11	2.22E+06	2.1%	0.61	0.81
	1.00E-10	2.31E-10	9.98E+05	3.31E-10	9.99E+05	21%	-0.09	0.30
	2.65E-10	3.36E-10	5.57E+05	6.01E-10	5.58E+05			
circular orbit	2.64E-10	2.12E-10	1.09E+06	4.76E-10	7.29E+05		0.00	0.00

Note: the equation solving was done by using Wolfram Alpha.

II-f. Using a 1D wave packet to describe a (position localized) photon, and to correlate the forming and emitting of this 1D wave packet to the electron’s orbital movement

In the text books, the 1D wave of an electromagnetic wave is generally explained with a transverse wave (see Giancoli p819, Figure 31-9, also see Figure 7e in current paper). In principle, the description of an emitted photon (or the orbital moving electron, or any motion particle) will become more accurate (in turns of its position) if we use a 1D matter wave packet (that is composed of many 1D waves with different frequencies). Here we try to use a 1D wave packet to describe an emitted photon (from H-atom’s n=3 to n=2 transition). To do that, we first simplified (or mimic) the n=3 orbital frequency ($f_{3,ph}=3.66E+14$ Hz) to be $f_{3,ph}=36$ Hz, the n=2 orbital frequency ($f_{2,ph}=8.22E+14$ Hz) to be $f_{2,ph}=82$ Hz, and the photon’s frequency ($\Delta f = 4.57E+14$ Hz) to be $\Delta f = 46$ Hz (notice that it come from $\Delta f = 82$ Hz -36 Hz =46 Hz). After many tests, we found that the wave packet that constructed by fixing the middle $f=46$, and averaging $y = -\cos(f/46*x)$ from $f = 23$ to $f= 69$ (with $\Delta f = 46$), with the step size $\delta f = 1$ (or 0.5, or 2, doesn’t matter) gave the most reasonable result (see Figure 6a). (Note: although any sine or cosine wave can be used for constructing the wave packet, we found the $-\cos(f/46*x)$ constructed wave packet can be explained most easily; Note: the formula $-\cos(f/46*x)$ defined that the base wave frequency is 46 Hz). The criteria that we used to judge whether it is a good wave packet are: **1)** the shape of the wave packet should be well converged (in Figure 6a, the main packet (represented by the orange dotted line) is within -1.5π to $+1.5\pi$, or within 1.5 wavelength at $f=46$ Hz); **2)** the center one full wave (from $-\pi$ to $+\pi$, see the red thick line in Figure 6a) of the wave packet should have frequency around 46 Hz. In Figure 6a, the grey-dot-thin line of $-\cos(x) = -\cos(46/46*x)$ defines that one wave (with wavelength from $-\pi$ to $+\pi$) has frequency of 46 Hz, the black-solid-thin line represents the main part of the wave packet (from -3π to $+3\pi$, or only showed 3 wavelengths of $f=46$ Hz), and the red-solid-thick line represents one full wave of the wave packet (from $-\pi$ to $+\pi$, or one wavelengths of $f=46$ Hz). Thus, the center one full wave of the (constructed) wave packet (in red-soli-thick line) has the frequency of 46 Hz.

Using the 1D wave packet, we can show the position and the size of a photon’s transverse wave. For example, by using the outline of the wave packet (i.e., the outline of the orange-dot-line in Figure 6a) to confine a delocalized (meaning

no starting point, no ending point on x-axis) 1D transverse wave (as shown in Figure 7e), we obtained a localized 1D transverse wave packet that is confined within $-1.5\pi \leq x \leq 1.5\pi$, or a size about 1.5 wavelength (at $f=46$ Hz).

Now we try to estimate that in Figure 5b, the orbital motion electron at what orbital position (before arriving the perihelion point) starts to emit the photon, and at what position (after passing the perihelion point) ends the emission of the photon. That is, to correlate the emission of the photon (i.e., the forming of its 1D wave packet) to the trajectory of the electron's orbital movement (in H-atom). (Note: we only need an approximation correlation, the perfect correlation is out of my capability). The first and the biggest approximation is, we assumed that the emitted photon's 1D wave packet has an effective size of one wavelength (this is based on the result that a $f=46$ Hz wave packet has the size about 1.5 wavelength shown in Figure 6a). For a $\lambda = 656.1$ nm photon (that emitted from H-atom's $n=3$ to $n=2$ transition), suppose it was generated at the perihelion point and passed through the same point at the speed of light, so it takes $\Delta t = \lambda/c = 6.561E-7$ (meters) / $3E+8$ (m/s) = $2.19E-15$ seconds to pass through the perihelion point (for the generation and emission of this photon).

1) Now let's consider the $n=3$ (circular orbital moving) electron in Bohr's H-atom, it has $r_{n=3} = 4.75E-10$ meters, $v_{n=3} = 7.29E+5$ m/s, and $n=3$ circular orbital circumference = $2\pi r_{n=3} = 2*3.14*4.75E-10 = 2.98E-9$ meters (see SunQM-6s1's Table 1). So, during $\Delta t = 2.19E-15$ s, the electron traveled (an orbital) distance = $v_{n=3} * \Delta t = 7.29E+5 * 2.19E-15 = 1.60E-9$ meters on a $n=3$ circular orbit. It equivalents to arc: $1.60E-9 / 2.98E-9 = \text{arc} / 2\pi$, $\text{arc} = 1.60E-9 / 2.98E-9 * 2\pi = 1.07\pi$, or about $1/2$ circle (of the $n=3$ circular orbit). Only half of that distance, or about $1/4$ circle, correlates to the first half of the photon generation and emission (before the $n=3$ electron reached the perihelion point).

2) Next, let's consider the $n=2$ (circular orbital moving) electron in Bohr's H-atom, it has $r_{n=2} = 2.12E-10$ meters, $v_{n=2} = 1.09E+6$ m/s, and $n=2$ circular orbital circumference = $2\pi r_{n=2} = 2*3.14*2.12E-10 = 1.33E-9$ meters (see SunQM-6s1's Table 1). So, during $\Delta t = 2.19E-15$ s, the electron traveled distance = $v_{n=2} * \Delta t = 1.09E+6 * 2.19E-15 = 2.39E-9$ meters on a $n=2$ circular orbit. It equivalents to arc: $2.39E-9 / 1.33E-9 = \text{arc} / 2\pi$, $\text{arc} = 2.39E-9 / 1.33E-9 * 2\pi = 3.59\pi$, or ~ 2 circles (of the $n=2$ circular orbit). Only half of that distance, or about one circle, correlates to the second half of the photon emission (after the electron passed the perihelion point and goes to the $n=2$ circular orbit). So, during the whole emission time ($\Delta t = 2.19E-15$ s), the electron (equivalently) spent half time in $n=3$ circular orbit for $1/4$ circle, then spent next half time in $n=2$ circular orbit for ~ 1 circle, (meaning, the emitted 1D wave packet is unsymmetrical).

3) Furthermore, if we use the pseudo-orbit at $n=2.433$ (see SunQM-6s1's Figure 1a), it has $r_{n=2.433} = 3.13E-10$ meters, $v_{n=2.433} = 8.99E+5$ m/s, and $n=2.433$ circular orbital circumference = $2\pi r_{n=2.433} = 2*3.14*3.13E-10 = 1.97E-9$ meters (see SunQM-6s1's Table 1). So, during $\Delta t = 2.19E-15$ s, the electron traveled distance = $v_{n=2.433} * \Delta t = 8.99E+5 * 2.19E-15 = 1.97E-9$ meters on a $n=2.433$ circular orbit. It equivalents to arc: $1.97E-9 / 1.97E-9 = \text{arc} / 2\pi$, $\text{arc} = 2\pi$, or exactly one circle. This is equivalent to say that the electron spends the half time on the first half circle of the $n=2.433$ circular orbit (before pass the perihelion point), and the half time on the second half circle of the $n=2.433$ circular orbit (after pass the perihelion point). It also means that the emitted wave packet is symmetric.

For an elliptical orbit, I (as a citizen scientist) am not able to do this kind of detailed calculation. However, according to Kepler's law, all elliptical (with different eccentricities, including the circular) orbits have the same orbital energy and the same orbital period as long as they have the same semi-major axis and radius (in QM, this means all these orbits have the same quantum number n , e.g., $|3,2,2\rangle$, $|3,2,1\rangle$, $|3,2,0\rangle$, $|3,0,0\rangle$, etc.). With this, we can reasonably say that **a photon's wave packet** (remember it has been assumed to be one full wave only) **generation and emission can be directly correlated to the electron moving for a one complete round of (elliptical/circular) orbit**, started from $|3,2,0\rangle$ elliptical orbit's aphelion site, to the (overlapped, or nearly overlapped) perihelion site of both $|3,2,0\rangle$ and $|2,1,0\rangle$ elliptical orbits, and then ended at the aphelion site of $|2,1,0\rangle$ elliptical orbit (see t_1 , t_3 , and t_5 points in Figure 5b).

Now let's analyze how the vectors of **electric field line \vec{E}** and the **magnetic field line \vec{B}** in 1D transverse wave correlates to the 1D wave packet and to the electron's orbital movement. (Note: see Appendix B for more explanations. Note: for simplicity, we first assume that the emitted photon's 1D wave packet is symmetric, as shown in Figure 7b).

4) In Figure 7b, at the start point t_1 (or $\theta = 0\pi$, or the aphelion point), \vec{E} vector (that always points from proton to electron) points upward along z-axis, so in Figure 7b's t_1 point (Note: t_1 is at the most right side of the x-axis), \vec{E} vector (the red arrow) also points upward;

- 5) When the electron moved to t_2 point (equivalent to $\theta = -\pi/2$ at a circular orbit in xz -plane, or similar as that in Figure 5b), the projection of \vec{E} on the z -axis is (about) zero, so the \vec{E} vector in Figure 7b is zero;
- 6) When the electron moved to t_3 point (equivalent to $\theta = -\pi$, or perihelion point), the projection of \vec{E} on the z -axis is negative maximum, so the \vec{E} vector in Figure 7b is also downward maximum;
- 7) When the electron moved to t_4 point (equivalent to $\theta = -3\pi/2$ at a circular orbit), the projection of \vec{E} on the z -axis is (about) zero, so the \vec{E} vector in Figure 7b is zero;
- 8) When the electron moved to t_5 point (equivalent to $\theta = -2\pi$, or aphelion point), the projection of \vec{E} on the z -axis is positive maximum, so the \vec{E} vector in Figure 7b is also upward maximum;
- 9) For the \vec{B} vector, because the electron is always moving anti-clockwise in xz -plane, or the \vec{E} vector is always rotating anticlockwise in xz -plane, thus, \vec{B} vector point to $-y$ direction (according to the right-hand rule). However, during the photon emission, the electron decelerated significantly at the perihelion region, it is equivalent to that the \vec{E} vector is accelerating clockwise (in xz -plane) at the perihelion region, thus, it caused \vec{B} vector to point to $+y$ direction temporarily (also according to the right-hand rule). This perfectly explained why \vec{B} vector oscillates in $\pm y$ directions in the 1D transverse wave.

This analysis showed that how the changing of \vec{E} vector and \vec{B} vector in 1D transverse wave correlates to the electron's orbital movement in a H-atom. (Notice that many times we have to mix the elliptical orbit with the circular orbit (on purposely) for the easier explanation).

One more thing we need to explain. According to the above explanation, during the first half of photon emission, the electron was mostly at the (equivalent) $n=3$ orbit (that has a relatively lower circular orbital frequency $f_{3,ph} = 3.66E+14$ Hz), and during the second half of photon emission, the electron was mostly at the (equivalent) $n=2$ orbit (that has a relatively higher circular orbital frequency $f_{2,ph} = 8.22E+14$ Hz). From a photon's momentum $p = \frac{h}{\lambda} = \frac{hf_{ph}}{c}$ (see Giancoli, p993, eq-37-5), it can be translated as the first half of photon's wave packet has a lower frequency, and the second half of photon's wave packet has a higher frequency (as shown in Figure 7a). Thus, a just emitted (or a newborn) photon has an unsymmetrical 1D wave packet. (Note: in Figure 6b, the un-symmetrical effect of the curve was drawn artificially, not a calculated result). After propagating for a while, the newborn photon's initial un-symmetry character will be eliminated (by QM's uncertainty principle force) to become a matured photon (with a symmetrical wave packet, see section II-i for detailed explanation).

From Figure 6a, we can see that a photon's 1D wave packet has a (effective) size around 1~3 wavelength of the photon. This is a very important result. We will use this result many times in the future. (Note: For a more advanced simulation, we should use Gaussian wave packet (see [27])). However, it is beyond my current calculation capability).

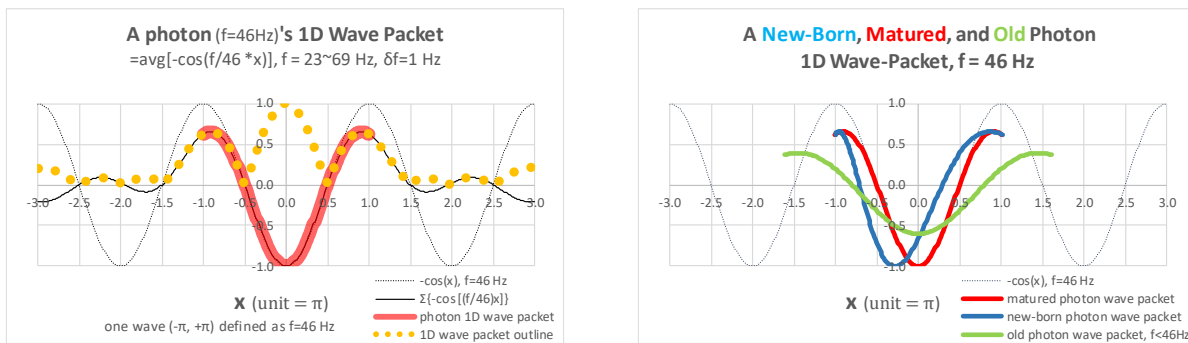


Figure 6a (left). A photon's 1D wave packet, calculated and plotted by using MS Excel. In the plot, one wave ($-\pi \leq x \leq \pi$) is defined as $f=46$ Hz. (Note: In calculation, all amplitude =1, no Gaussian distribution for amplitude).

Figure 6b (right). Illustration of the 1D wave packet for a newborn photon (in blue), a matured photon (in red), and an old photon (in green). (Note-1: the newborn wave packet is artificially drawn, not a calculated curve. Note-2: even it is unsymmetrical, the center one-wave part (or the dominant part) of the newborn wave packet has its one full-wave covers $\pi \leq$

$x \leq \pi$, which means $f \approx 46$ Hz. This determined the principle frequency of the whole wave packet (even it has a big variance range of frequency)).

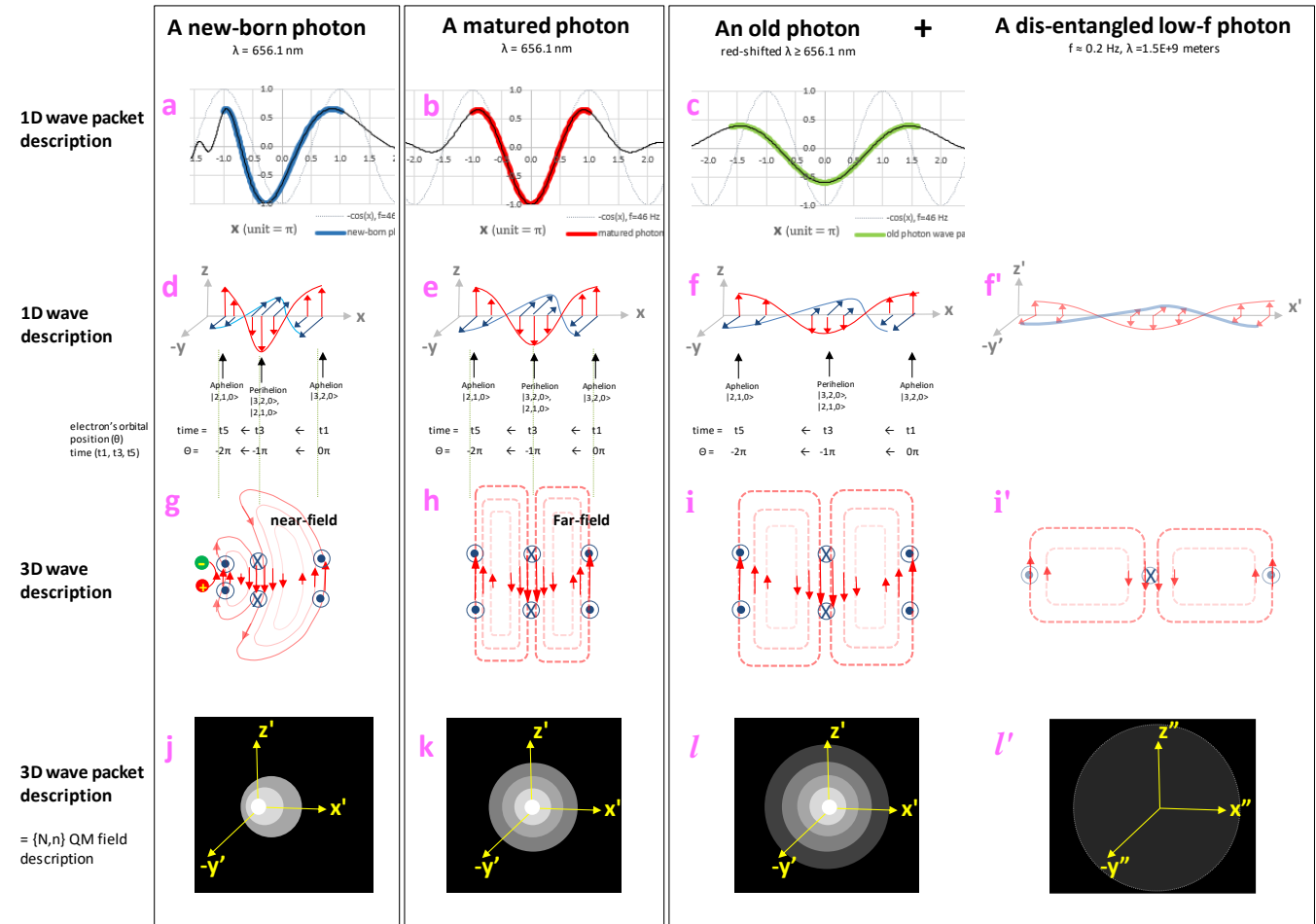


Figure 7. Unification of all four different kind of wave explanations (1D-wave, 1D-wave packet, 3D-wave, and 3D wave packet) for the photon emission and propagation, and also correlated it to the electron's orbital movement in H-atom.

Figure 7 (a, b, c). Illustration of 1D wave packet of a newborn photon, a matured photon, and an old photon.

Figure 7 (d, e, f, f'). Illustration of 1D (transverse) wave of a newborn photon, a matured photon, and an old ("decaying") photon.

Figure 7 (g, h, I, I'). Illustration of 3D wave of a newborn photon, a matured photon, and an old photon.

Figure 7 (j, k, l, l'). Illustration of 3D wave packet of a newborn photon, a matured photon, and an old ("decaying") photon.

II-g. Using the antenna theory to design a 3D wave description for an emitted photon

For a photon's wave description, so far we have the 1D wave description, the 1D wave packet description, and we would like to have a 3D wave description. In the text books, the 3D wave of an electromagnetic wave is generally explained with the antenna theory (see Giancoli, page 818). Thus, we may only need to modify the antenna theory for the purpose of photon description.

Started from the antenna theory, a dipole oscillation (along z-axis) may can be mimicked by the $|nL0\rangle$ elliptical orbit movement at the eccentricity $e \approx 1$. So we may can directly use the $|nL0\rangle$ elliptical orbit model to describe the electromagnetic wave antenna/receiver knowledge, and then to further describe the 3D wave of an emitted photon. Let's still use H-atom's $|3,2,0\rangle$ extreme elliptical orbit as the example. When an electron moves from aphelion to perihelion (in xz-plane, from 0π to $-\pi/2$ to $-\pi$, anti-clockwise, see Figure 4b that has $e \approx 1$, so it is in nearly z-1D movement, also see Figures 8a ~ 8f), it can be simplified as driven by the +/- charge's attractive force. Its (practically 1D on z-axis) dipole change (acceleration followed by deceleration) produced a half electromagnetic wave (or a half "photon", because we now know that one photon contains one (full) wave of 1D wave packet) "emitted" along x-axis (shown in Figure 8c', with the whole process shown in Figure 8 (a', b', c')). Notice that at the perihelion site, the electron is always closest to the proton. Then, what is the driving force to make this electron goes back to the aphelion point? Well, it (like a receiver) absorbs the just "emitted" half "photon" completely (this complete absorption or quantum absorption may can be attributed to the QM-force), and use that energy to drive the electron to move away from the proton and going back to the aphelion point, see Figure 8 (c', d', e', f'). Thus, this whole cycle has no energy lost, no true emission of "photon", and the cycle can be repeated again and again. (Note: in this explanation, we mixed the z-1D dipole movement and xz-2D elliptical orbital movement on purposely for easier explanation. Note: In this case, the electron always stays in $|3,2,0\rangle$ orbit, no orbital transition. The regular kinetic/potential energy conversion is re-explained by the half "photon" emission and half "photon" absorption cycle).

In the case of $|3,2,0\rangle$ to $|2,1,0\rangle$ transition, the aphelion point of $|2,1,0\rangle$ is closer to the proton than that of $|3,2,0\rangle$, so the electron only need to use part energy of the first half "emitted photon" to go to the aphelion of $|2,1,0\rangle$, the rest part energy of the first half "photon" is truly emitted (as the first half of a 656.1 nm photon). The acceleration followed by deceleration of the electron from perihelion to aphelion in $|2,1,0\rangle$ orbit (in xz-plane, from $-\pi$ to $-3\pi/2$ to -2π , anti-clockwise) add the second half wave of the 3D wave (of the 656.1 nm photon) that is truly emitted, see Figure 8 (d'', e''). Thus, in the one (full) wave of a just truly emitted (656.1 nm) photon's 3D wave, the first half wave (on the right side) is more extended than the second half of the wave (on the left side, see Figure 8f''). Therefore, like that in the 1D wave and 1D wave packet description, a newborn photon's 3D wave is unsymmetrical. It is almost the same as the antenna radio wave's near-field, except that it propagates only in +x direction. In Figure 7g (that equals to Figure 8f'''), the \vec{E} vector and the \vec{B} vector at each phase of the 3D wave were also shown, and they have the exactly the same phase as that shown in the 1D wave description (Figure 7d). Notice that in Figure 7g, only one frequency of a 3D wave mode of a photon was illustrated. There are many different frequencies of 3D wave modes emitted simultaneously (all in the same x-direction), and the whole collection of these modes forms a real photon (see the 3D wave packet description of a photon in the next section).

In Figure 7h we drew a matured photon's 3D wave. Notice that the un-symmetry character (of the newborn photon) is diminished. Thus, like that in the 1D wave and 1D wave packet description, a matured photon's 3D wave is symmetrical. It is almost the same as the antenna radio wave's far-field, except that it propagates only in +x direction. The \vec{E} vector and the \vec{B} vector at each phase of the 3D wave were also drawn in Figure 7h, and they have the exactly the same phase as that shown in the 1D wave description (Figure 7e, also see Giancoli's p818, Figure 31-8).

Then, what is the difference between a photon's 3D wave emission and a radio wave's 3D wave radiation? The only difference is that in a photon's 3D wave radiation, there is only one 3D wave packet emitted in a single (+x) direction, while in a radio wave's 3D wave radiation, there are many 3D wave packets emitted simultaneously in all directions (within xy-plane). Thus, we (conceptually) unified the 3D wave explanation for a photon emission and a radio wave radiation.

The photon's 3D wave model is still in the early phase of designing and developing. There are still many unknowns:

- 1) Here we tried to use the concept that both the electric field and magnetic field should follow the Schrodinger equation (see SunQM-6), although we haven't figured out the details. For example, how to use Schrodinger equation's wave function field (in the non-Born probability (NBP) form) to describe a newborn photon's 3D wave?
- 2) Based on Figure 8, to generate and emit a 656.1 nm photon, does the electron need to do one complete orbital movement (half orbital movement from $|3,2,0\rangle$ orbit's aphelion to perihelion, then half orbital movement from $|2,1,0\rangle$ orbit's perihelion to aphelion), or does the electron need to do more than one complete orbital movement? We are not 100% sure about this.
- 3) It is possible that we may re-design part of the description in the future. As a former bench scientist (biophysicist), for every experiment I did, I needed to first design it, and then to test it. Re-designing and re-developing was my routine work before the success (especially for the global fitting, see SunQM-7's Appendix G).

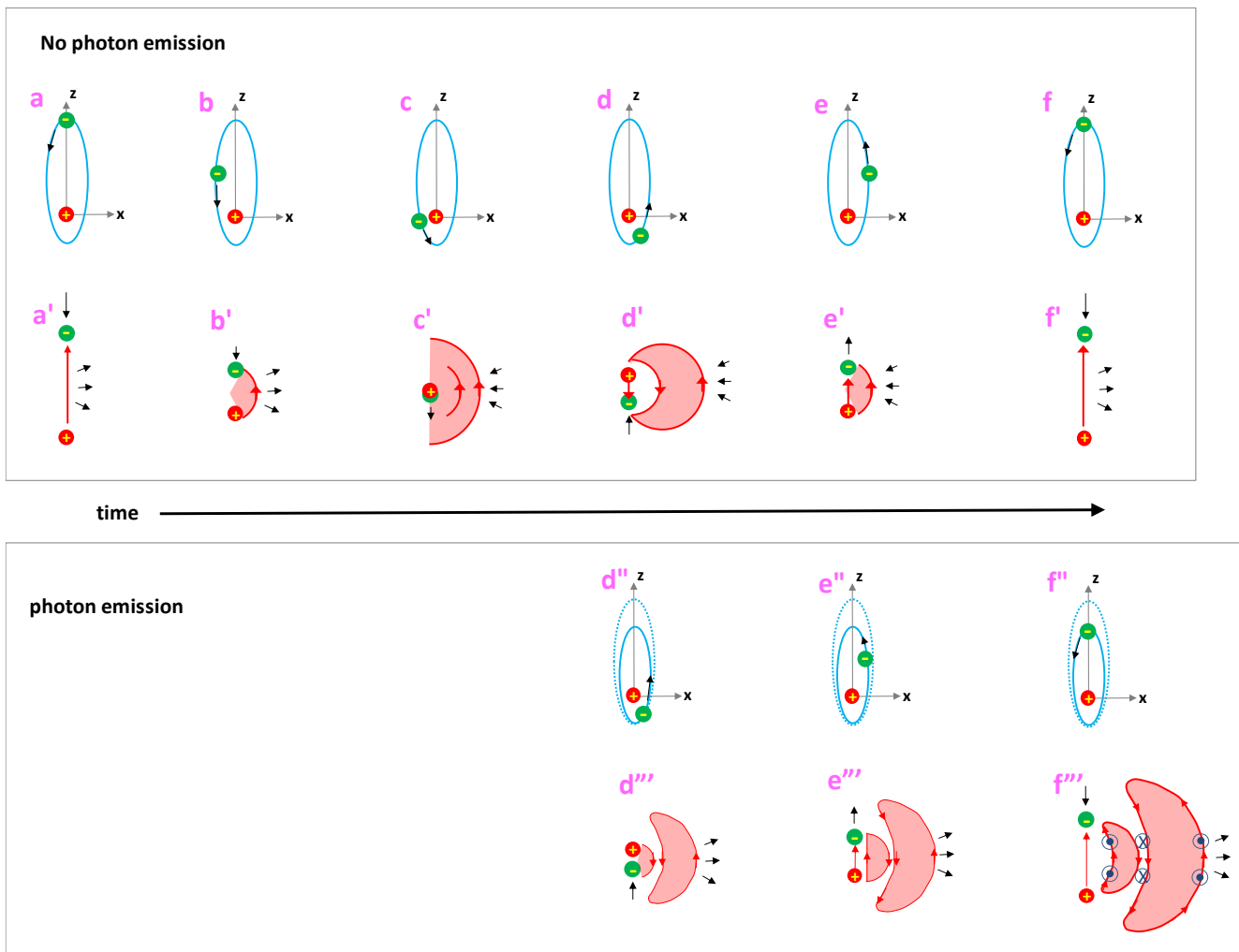


Figure 8. Illustration of the formation and emission of a photon's 3D wave. The blue lined ellipses represent the elliptical orbit of the electron in a H-atom. The red lines represent the electric field line. Time progresses from Figure-a up to Figure-f. All figures that have the same letter (e.g., d, d', d'', d''') are at the same time point.

Figure 8 (a, b, c, d, e, f). An electron is orbiting a proton along an elliptical orbit (in xz-2D). No orbital transition. It can be degenerated as a +/- charge dipole oscillates along z-axis.

Figure 8 (a', b', c', d', e', f'). The dipole oscillation produced electromagnetic 3D-wave emission and re-absorption. The red-shadow represents the energy that has been "emitted" and then re-absorbed by the dipole (to drive the electron away from the proton from perihelion to aphelion).

Figure 8 (d'', e'', f''). During $|3,2,0\rangle$ to $|2,1,0\rangle$ orbital transition, the electron moves less distance from the perihelion back to the aphelion.

Figure 8 (d''', e'''). Thus, only part energy of the first half "emitted photon" is absorbed, the rest part energy of the first half "photon" is truly emitted as the first part of a newborn photon. Notice that the crescent shape came from the Figure 8d'.

Figure 8f'''. A (fully formed and emitted) newborn photon that emitted in x-direction.

II-h. Using the $\{N,n\}$ QM field structure for the 3D wave packet description of an emitted photon

Now, we have the 1D-wave description, the 1D-wave packet description, and the 3D wave description for a photon. This immediately promotes us to looking for the 3D-wave packet description for a photon. This also forced us to think how the $\{N,n\}$ QM field description of a photon's physical structure (see SunQM-6s1's Figure 4a) can be fitted into this whole big picture. All the sudden, I realized that the $\{N,n\}$ QM field description of a photon's physical structure (in SunQM-6s1's Figure 4) is exactly the 3D wave packet description of a photon.

In Figure 7j we drew a newborn photon's 3D wave packet. It is similar as what we had drawn in SunQM-6s1's Figure 3. We believe that it should can be described with Schrodinger equation's wave function field (in the non-Born probability (NBP) form), and in the many frequency modes. It must be the Fourier combination of all these (many different frequency 3D waves) modes that formed the 3D wave packet (Note: Sorry, as a citizen scientist, I don't have the ability to prove it mathematically). Like that in the 1D wave packet, the effective size of the 3D wave packet of a photon is also around 1~3 wavelength of the photon. (Note: We believe that one wavelength is the minimum size of a photon's 3D wave packet can have. If the effective size of a photon's 3D wave packet is smaller than one wavelength of the photon (e.g., half wavelength), then the frequency of this photon becomes too variable or even uncertain).

As a (over) simplified description, we can treat each shell or core (of a photon's 3D wave packet) as a single component that has a size of one wavelength, so that the core component has the shortest wavelength (or the highest frequency), the inner shells have the medium wavelengths (or the medium frequencies), and the outer shells have the longest wavelengths (or the lowest frequencies). In this way, we can describe a photon's 3D wave packet as that its core has the highest frequency, and its outmost shell has the lowest frequency, and all shells are entangled with each other and with the core to form a single entity (of a 3D wave packet).

Also, we see that 3D wave packet has a character of forever size-growing: as it propagates (from $|2,1,1\rangle$, to $|3,2,2\rangle$, then to $|4,3,3\rangle$, $|5,4,4\rangle$, etc., see SunQM-6s1's Figure 3), its size is keep increasing. Also, like that in the 1D wave, 1D wave packet, and 3D wave description, a newborn photon's 3D wave packet is also unsymmetrical.

In Figure 7k we drew a matured photon's 3D wave packet. Again, we believed that it can be described with Schrodinger equation and NBP, and it is the Fourier combination of many 3D waves (each with different frequencies). It still keeps the forever size-growing character. Like that in the 1D wave, 1D wave packet, and 3D wave description, a matured photon's 3D wave packet is also symmetrical (see the next section for more explanation). Interestingly, in SunQM-6s1's Table 2, we had calculated out that for a $\lambda = 656.1$ nm photon (that emitted from a H-atom), how far it propagates before changed from an unsymmetrical shape to a symmetrical shape: "when a (hydrogen atom) emitted photon propagated to $n = 6^{\wedge}5$, or about 3 mm away, it became a spherical shape (at 10% peak max, under the $\{N,n\}$ QM field description)".

Further propagation continues increase the size of the 3D matter wave packet, and, after passing a certain critical point (that correlated the Hubble constant ~ 70 (km/s)/Mpc), the over-sized outmost shell of the 3D matter wave packet is trimmed-off (or split-out, or bumped-off), and caused a propagating photon lost a tiny amount of energy, and produced a cosmic red-shift (see Figure 7l and Figure 7l').

Thus, we (conceptually) unified all four different kind of wave explanations (1D-wave, 1D-wavepacket, 3D-wave, and 3D wave packet) for the newborn photon, the matured photon, and the old photon, and also correlated it to the electron's orbital movement in H-atom (that generated this photon, see all figures in Figure 7).

Based on above result, we may can describe a 656.1 nm photon's 3D wave packet as that it has a dominant shell with diameter of 656.1 nm (and frequency of $4.57E+14$ Hz), and there are several inner shells and one core that have shorter wavelengths or higher frequencies, and there are several outer shells that have longer wavelengths or lower frequencies. When the outmost shell grows its size to $r = 2.7E+10$ meters (see next section), it will be dis-entangled from the main body of the photon, and become a newborn low-f (0.02 Hz) photon. (Note: The core size of a 656.1 nm photon may can be estimated to be $r = 2.57E-24$ meters. It was calculated as, a 656.1 nm photon has $\Delta f_{ph} = 4.57E+14$ Hz, $E = h \Delta f_{ph} = 3.03E-19$ J = 1.89 eV. Check SunQM-7's Table 1, a 1.89 eV/c² particle may stay in $\{-21,2//6\}$ QM state, and may have the size of $\{-21,3//6\}$. Then, check SunQM-5's Table 1, a $\{-21,3//6\}$ size has radius at 9x of that at $\{-21,1//6\}$, or $r = 9 \times 2.86E-25 = 2.57E-24$ meters).

II-i. The uncertainty principle may be the driving force to symmetrize a newborn photon, and also to red-shift an old photon.

We believe that the uncertainty principle ($\Delta p \Delta x \geq \hbar/2$) may should be used to explain why a newborn (un-symmetrical) photon, after propagation for a while, automatically becomes a symmetrical photon. According to de Broglie's formula, a photon has momentum $p = \frac{h}{\lambda} = \frac{hf_{ph}}{c}$. (Note: According to SunQM-6s1's eq-11, light speed is a phase velocity, not a group velocity. Then, according to $v_{gr} = 2 * v_{ph}$, a photon's group velocity should have two times of light speed ($2c$). Also notice that the wave front of a propagating photon (with the light speed c) should have two times of light speed ($2c$). However, according to a text book [28], electromagnetic wave has $v_{gr} = v_{ph}$. Based on it, we assumed here that a photon propagation also has $v_{gr} = v_{ph}$. However, this still remains as an unsolved problem). During the whole photon emission process, (within one orbital circle), the orbital moving electron gradually (or quantumly? or rapidly?) loss its orbital momentum, initially by zero, finally increased to $1.01E-27 \text{ kg}\cdot\text{m/s}$ (= (electron's mass) multiplies Δv (=1109 m/s)). So the just emitted (newborn) photon has the momentum variance from 0 to $1.01E-27 \text{ kg}\cdot\text{m/s}$ (or λ variance from ∞ to 656.1 nm. Notice that this momentum change associated with zero mass). This large momentum variance gives the larger momentum uncertainty (Δp). Also, the just emitted photon has the smallest size (relative to its forever growing size during the propagation), so its position uncertainty (Δx) is the smallest. Here we hypothesized that the forever size-growing is the natural attribute of a propagating photon. We also hypothesized that for a propagating photon, the uncertainty principle ($\Delta p \Delta x \geq \hbar/2$) will keep the product of $\Delta p \Delta x = \text{constant}$. Then, after propagated for a while, the size of the photon is increased (that can be translated as the position uncertainty Δx of this photon is increased). It forces this propagating photon to decrease its Δp . The smaller Δp means the photon has less frequency variance, thus its 3D (or 1D) wave packet is more symmetrical. After the un-symmetry of the 3D wave packet is diminished enough, the photon is said to be "matured".

Then, during the further propagation (after the propagating photon has matured), the size of the symmetrical photon (of the 3D or 1D wave packet) grows continuously (and so does its Δx uncertainty). Then, after Δx passed a critical point (that correlated the Hubble constant $\sim 70 \text{ (km/s)/Mpc}$), the amount of Δp decreasing become limited and can no longer compensate the amount of Δx increasing (to keep the $\Delta p \Delta x = \text{constant}$), then the uncertainty principle-force starts to trim-off the over-sized part (i.e., the low-frequency end) of the 3D (or 1D) symmetric wave packet (to form a new low-f 3D (or 1D) wave packet), and causes a propagating photon to loss a tiny amount of energy, and produced the red-shift for a propagating photon. At this time, the photon is said to be "old" and red-shifted. This trimming process repeated again and again, produced the cosmic red-shift of an old photon.

Alternatively, if we treat the red-shifted photon (i.e., the main body) and all the (continually) trimmed-off low-f photons as one entity, then this entity will have even larger position uncertainty Δx as it propagates (due to that the low-f photons may be bumped-off at random directions). As more and more low-f photons trimmed-off (at different directions), the position uncertainty Δx of this entity keeps growing forever.

From an even bigger picture, we can think that:

- 1) A free neutron's 3D wave packet is always growing. After passed a critical point (where its Δp decreasing become limited and can no longer compensate the amount of Δx increasing to keep the $\Delta p \Delta x = \text{constant}$), this free neutron decays into a proton, an electron and an antineutrino. If we treat these three particles as one entity, as this entity propagated, its position uncertainty Δx grows forever. Notice that a neutron's beta-decay has only one-time splitting, while a photon's red-shift has many-times splitting.
- 2) A nuclear fission may can be treated exactly the same way as above.
- 3) A planet formation (i.e., accretion of many orbital fragments to form one planet), a star formation (i.e., a nebula collapse), or a black body formation (i.e., a star collapse), they all have the position uncertainty Δx (of the combined mass distribution) decreasing (under the influence of the gravitational force).
- 4) From above discussions, we may hypothesize that, **4a**) a massless energy 3D wave packet (e.g., a photon) will have Δx uncertainty continuously increasing followed by the continually trimming-off the (over-sized) low-f photons; **4b**) a small-mass particle may have Δx uncertainty continuously increasing followed by a (one-time) body-splitting; **4c**) a large-mass "particle" may have Δx uncertainty continuously decreasing (rather than increasing). So, it is the mass of a particle/object that determines the Δx uncertainty (of this particle/object) to increase or decrease (along with time).

5) If this hypothesis is correct, then, a neutrino, if it is massless, will keep trimming-off its energy continually (like an old photon does). For any massless (pure energy) particle (like a photon that is composed of pure E/RFe energy wave packet, or a graviton that is composed of pure G/RFg energy wave packet, or a gluon that is composed of pure S/RFs energy wave packet), its size may be always increasing as propagating, and the uncertainty principle ($\Delta p \Delta x = \text{constant}$) may trim the forever size-growing Δx , and thus cause the red-shift. Therefore, it is possible that the same cosmic red-shift will apply to a free propagating graviton and/or a gluon.

6) For a massless mega-“photon” (see SunQM-7’s section V, and SunQM-5s1’s Appendix), the possible forever size-growing of Δx and the trimming of Δx (by $\Delta p \Delta x = \text{constant}$) may cause the red-shift of mega-“photon” to be the CMB. (Note: There are two possible ways: **6a**, the majority part of the mega-“photon” became the mass (i.e., the hydrogen), the residue part of the mega-“photon” red-shifted to be the CMB; **6b**, all mega-“photon” became the mass, the CMS is the low-f photons that the mega-“photon” spitted-off right before it became mass). Actually, a mega-“photon” may be a pure energy of a mega-“particle” with the mixture energy of E/RFe, G/RFg, and S/RFs. We will not have the capability to detect the CMB of G/RFg and/or S/RFs for at least hundreds of years.

All discussions in this section are try to support the following hypothesis: **it is the natural attribute of an old photon to produce the red-shift. Nothing peculiar. Thus, the “(explosive-like) major expanding Universe” model may not be needed to explain the cosmic red-shift.** However, it does not contradict with a “(breath-like) minor expanding/contracting Universe” model (see SunQM-7’s Figure 6c). (Note: All these are only a citizen scientist-leveled discussion).

In SunQM-6s1’s Table 5, we had estimated the possible frequency value of a low-f photon with the assumption that a propagating photon’s (spitted-out) outmost shell may have a size of 100 wavelength (notice that this 100 was an arbitrarily guessed number). Now using the result of current section, we can reasonably to assume that **a propagating photon’s (spitted-out) outmost shell has an effective size of one wavelength.** Under this new condition, the same calculation (as in SunQM-6s1’s Table 5) showed that (to satisfy Hubble constant ~ 70 (km/s)/Mpc), a 656.1 nm photon, after propagating each $\sim 2.7E+10$ meters (about a half distance from Sun to Mercury), it will split-out a **0.02 Hz low-f photon.** Further estimation showed that a 656.1 nm photon (that emitted from a H-atom in the Sun), when arrived to Earth, it would have split-out low-f photon five times, each time with a single 0.02 Hz low-f photon. When this 656.1 nm photon arrived to Earth, it will have red-shifted by $\Delta \lambda \approx 1.4E-13$ nm (calculate by using WolframAlpha).

(Note: If we assume that a propagating photon’s (split-out) outmost shell has an effective size of three wavelengths, then a 656.1 nm photon is estimated to split-out a 0.04 Hz low-f photon after propagating each $\sim 2.7E+10$ meters).

We may can say that it is the uncertainty principle that caused the forever growing of a propagating photon (by increasing Δx), and it is also the uncertainty principle (formed QM force) that trimmed the over-sized photon (by enforcing $\Delta p \Delta x = \text{constant}$, while limiting the decreasing of Δp). So the uncertainty principle may be the driving force for the red-shift of a propagating photon. (Note: Another important function of the uncertainty principle (e.g., $[L_x, L_y] = i\hbar L_z$, $[L_y, L_z] = i\hbar L_x$, $[L_z, L_x] = i\hbar L_y$, etc.) is that it may directly equal to the rotation diffusion (or RotaFusion, or RF, see SunQM-6’s section 6)). Unfortunately, as a citizen scientist, I don’t have the mathematical ability to prove these hypotheses.

If the low-f photon hypothesis is correct, then our universe is full of these low-f photons (with different frequencies but all in sub-Hz frequency range). Our current technology is not able to detect this kind of sub-Hz photons. The main difficult is that because their wavelength is too large (or each of these 3D wave packet takes very large space), there are always many (different frequencies of) sub-Hz photons share the same space at any specific time, so that you can never single one out of the rest (to measure it).

II-j. Some calculations to show that under the “ $|nL0\rangle$ elliptical orbital transition model”, we can treat the ($\lambda=656.1$ nm) photon as a low-frequency (or low-f) outmost shell of an orbital moving electron’s 3D wave packet that is disentangled (or spun-off) during the orbital transition from $|3,2,0\rangle$ to $|2,1,0\rangle$

(Note: in this section, m means mass, not the quantum number). First, in the general calculation of momentum ($p = mv$) and the kinetical energy ($K = \frac{1}{2} mv^2$) for a particle or a celestial body, we always use the $v_{\text{classical}} = v_{\text{gr}}$, not use the v_{ph} . So, strictly, we should write

$$p = mv_{\text{gr}} \quad \text{eq-11a}$$

$$K = \frac{1}{2} mv_{\text{gr}}^2 \quad \text{eq-12a}$$

Then, for a matter wave, $v_{\text{classical}} = v_{\text{gr}} = 2v_{\text{ph}}$ (see SunQM-6s1's eq-1), or $\frac{1}{2}v_{\text{gr}} = v_{\text{ph}}$, plus using $v_{n,\text{ph}} = \lambda_n f_{n,\text{ph}}$ (see SunQM-6s1's eq-11), and de Broglie formula $p = h/\lambda$, we obtain the wave-particle duality form of the momentum and kinetical energy formulas:

$$p = h/\lambda \quad \text{eq-11b}$$

$$p = hf_{\text{ph}}/v_{\text{ph}} \quad \text{eq-11c}$$

$$K = mv_{\text{gr}} v_{\text{ph}} \quad \text{eq-12b}$$

$$K = p v_{\text{ph}} \quad \text{eq-12c}$$

$$K = p \lambda f_{\text{ph}} \quad \text{eq-12d}$$

$$K = (h/\lambda) \lambda f_{\text{ph}} = hf_{\text{ph}} \quad \text{eq-12e}$$

$$mv_{\text{gr}} v_{\text{ph}} = hf_{\text{ph}} \quad (\text{after combining eq-12b with eq-12e}) \quad \text{eq-12e'}$$

Although for electron and other matter, $v_{\text{gr}} = 2v_{\text{ph}}$, but for photon, $v_{\text{gr}} = v_{\text{ph}}$, see [28], then we have

$$p_{\text{photon}} = hf_{\text{ph}}/v_{\text{ph}} = hf_{\text{gr}}/v_{\text{gr}} \quad \text{eq-11d}$$

Notice that eq-11a through eq-11c are the isoforms of the same formula for momentum, and eq-12a through eq-12e are the isoforms of the same formula for the kinetical energy. Also notice that in an elliptical orbit, the transient orbital momentum of an object can be transformed into $mv_{\text{gr}} = hf_{\text{ph}}/v_{\text{ph}}$, or, $mv_{\text{gr}} v_{\text{ph}} = hf_{\text{ph}}$, which is the orbital kinetical energy formula of either eq-12b or eq-12e. Therefore, in an elliptical orbit, the transient orbital momentum has the isoform formula as that of the orbital kinetical energy. (Note: eq-11a through eq-11c, and eq-12a through eq-12e, should go together with SunQM-6s1's eq-1 through eq-22).

Then, for the circular orbital (bound) energy $E = K + V = -\frac{1}{2} mv_{\text{gr}}^2$, (where V is the potential energy, ignored the reduced mass, meaning the center object's mass is much bigger than the orbital object's mass, see SunQM-2's eq-2), we have

$$E_{\text{orbit}} = K_{\text{orbit}} + V_{\text{orbit}} = -\frac{1}{2} mv_{\text{gr}}^2 = -hf_{\text{ph}} \quad \text{eq-13}$$

Or,

$$E_{\text{orbit}} = -hf_{\text{ph}} = -(h/m') m f_{\text{ph}} = -Hmf_{\text{ph}} \quad \text{eq-14}$$

Thus, eq-14 is the same as SunQM-6s1's eq-13. (Note: For the meaning of H and m' , see SunQM-2's section II-c).

Explanation-1: Using $|nL0\rangle$ elliptical orbit's transient velocity at the perihelion site to explain:

In the " $|nL0\rangle$ elliptical orbital transition model", we should can treat a ($\lambda=656.1$ nm) photon as a low-frequency (or low-f) spin-off of an elliptical orbital moving electron. To show it, we need to use the transient orbital momentum of the electron ($p = mv_{\text{gr}} = h/\lambda = hf_{\text{ph}}/v_{\text{ph}}$, or $f_{\text{ph}} = mv_{\text{gr}}v_{\text{ph}}/h$, which equivalent to use the transient orbital kinetic energy of the electron $K = m v_{\text{gr}} v_{\text{ph}} = hf_{\text{ph}}$), to calculate the transient elliptical orbital frequency of the electron at the perihelion. Here, we still use the model in section II-d (at the perihelion site, $\Delta\vec{p} > 0$ and $\Delta\vec{x} = 0$) as the example. Using the data in eq-5, we can calculate the transient orbital frequency at the perihelion of the $|3,2,0\rangle$ extreme elliptical orbit

$$f_{3,\text{ph},p} = mv_{3,\text{gr},p} v_{3,\text{ph},p} / h = \frac{1}{2} mv_{3,\text{gr},p}^2 / h = (1/2) * 9.109E-31 * (2.99550594E+8)^2 / 6.626E-34 = 6.1677909E+19 \text{ Hz.} \quad \text{eq-15}$$

$$\text{Similarly, we can calculate the transient orbital frequency at the perihelion of the } |2,1,0\rangle \text{ extreme elliptical orbit} \\ f_{2,\text{ph},p} = \frac{1}{2} mv_{2,\text{gr},p}^2 / h = (1/2) * 9.109E-31 * (2.99549485E+8)^2 / 6.626E-34 = 6.1677453E+19 \text{ Hz.} \quad \text{eq-16}$$

The difference of these two is

$$\Delta f_{3-2} = f_{3,ph,p} - f_{2,ph,p} = 4.57E+14 \text{ Hz.} \quad \text{eq-17}$$

This is exactly the ($\lambda=656.1$ nm) photon's frequency. Now, it is obvious that (we can say that) the $\lambda=656.1$ nm photon has the low-frequency (i.e., $4.57E+14$ Hz) in comparison to the frequency ($6.1677909E+19$ Hz) of the elliptical orbital moving electron at the perihelion site. Thus, we can treat the $\lambda=656.1$ nm photon as a low-f outmost-shell of an orbital moving electron that is dis-entangled (or spun-off) during the orbital transition. In other words, we can treat the $\lambda=656.1$ nm photon as the outmost-shell of an orbital moving electron's 3D wave packet that is spun-off at the perihelion site during the orbital transition. (Note: in this explanation, we should not use the circular orbit's frequency (shown in SunQM-6s1's Figure 1a). We have to use the transient elliptical orbital frequency at the perihelion site where the orbital transition or the photon emission is happening).

A second way to express the same concept is: a $|3,2,0\rangle$ elliptical orbit moving electron at the perihelion site (that equivalent to a (momentum) 3D wave packet) initially carried a transient $p = m_e v_{3,gr,p} = 9.109E-31 * 2.99550594E+8 = 2.7286064E-22$ (kg.m/s), then it spin-off a (tiny amount of momentum as a newly formed (momentum) 3D wave packet) with $p = m_e \Delta v_{3-2,gr,p} = 9.109E-31 * 1109 = 1.01E-27$ (kg.m/s) as a photon (with $p=h/\lambda$, or $\lambda = h/p = 6.626E-34 / 1.01E-27 \approx 656$ nm, notice that the photon's momentum contains zero mass), the rest momentum (with transient $p = 9.109E-31 * (2.99550594E+8 - 1109) = 2.7285963E-22$ (kg.m/s), also as a (momentum) 3D wave packet) is carried by a de-excited electron that transit to the $|2,1,0\rangle$ orbit.

A third way to express the same concept is: a $|3,2,0\rangle$ elliptical orbit moving electron at the perihelion site (that equivalent to a (kinetical energy) 3D wave packet) initially carried a transient kinetical energy $K = \frac{1}{2} m_e v_{3,gr,p}^2 = (1/2) * 9.109E-31 * (2.99550594E+8)^2 = 4.0867783E-14$ (Joule), then it spin-off a (tiny amount of kinetical energy in the new) 3D wave packet with $K = \frac{1}{2} m_e (v_{3,gr,p}^2 - v_{2,gr,p}^2) = 3.026E-19$ (Joule) as a photon (with $K = hf_{ph}$, or $f_{ph} = K/h = 3.026E-19 / 6.626E-34 = 4.57E+14$ Hz, or $\lambda = c/f_{ph} = 3E+8 / 4.57E+14 \approx 656$ nm), the rest kinetical energy (with the transient $K = (1/2) * 9.109E-31 * (299549485)^2 = 4.0867480E-14$ (Joule), also as a (kinetical energy) 3D wave packet) is carried by a de-excited electron that transit to the $|2,1,0\rangle$ orbit.

Explanation-2: Using Bohr circular orbit's constant orbital velocity to explain:

With the new knowledge that the 3D wave packet of a photon (that produced in (roughly) one round of the elliptical orbit that the electron moved) has a (effective) size around one wavelength of the photon (see Figure 7), now we can explain (more intuitively) that why the emitted photon is the outmost shell of an (orbital moving) electron's 3D wave packet. According to SunQM-7's Table 1, an electron with (rest) mass = $0.511 \text{ MeV}/c^2$ may have size at around $\{-17,1//6\}$, or with a radius no more than $6.48E-19$ meters (see SunQM-5's Table 1). Let's suppose this is the core size of a 3D wave packet of an electron. In Bohr circular orbit model, a $n=3$ electron has (the averaged) $v_{3,gr} = 7.29E+5$ m/s (see SunQM-2's Table 2) and the de Broglie matter wavelength $\lambda_{n=3} = h/(mv_{3,gr}) = 6.626E-34 / (9.109E-31 * 7.29E+5) = 9.98E-10$ meters. Meanwhile, a $n=2$ electron has the de Broglie matter wavelength $\lambda_{n=2} = h/(mv_{2,gr}) = 6.626E-34 / (9.109E-31 * 1.09E+6) = 6.67E-10$ meters. So, a large-sized 3D wave packet (diameter $\approx 9.98E-10$ meters for $n=3$ electron) spin-off its outmost shell to become a small-sized 3D wave packet (diameter $\approx 6.67E-10$ meters for $n=2$ electron). The spun-off outmost-shell become a new (low-f) 3D wave packet with wavelength (or the size) of 656 nm (calculates as $\Delta f = f_2 - f_3$, $f_3 = v_{3,ph} / \lambda_3 = v_{3,gr} / 2 / \lambda_3$, $\Delta \lambda = c/(f_2 - f_3) = c/(v_{2,gr} / 2 / \lambda_2 - v_{3,gr} / 2 / \lambda_3)$).

Explanation-3: Using $|nL0\rangle$ elliptical orbit's transient velocity at the aphelion site to explain:

Can we use the transient velocity at the perihelion site of the elliptical orbit for the same calculation (in the Explanation-2)? No. Because the transient $v_{3,gr,p}$ is faster than the transient $v_{2,gr,p}$, so the wavelength is smaller. Why not? This is because the real physical process of the photon emission starts form aphelion, maximum at perihelion, then end at aphelion. It is not only at perihelion site. So, physically, the fast orbital velocity near the perihelion site formed the high-frequency core of the emitted photon's 3D wave packet, while the slow orbital velocity at the aphelion site formed the low-frequency outmost-shell of the emitted photon's 3D wave packet. Therefore, to compare the size of the outmost shells, we should use the aphelion transient velocity rather than the perihelion transient velocity. The ($n=3$ and $n=2$) aphelion radii are calculated as

$$r_{3,ap} = 2 * r_{3,circular} - r_{3,p} = 2 * 4.763E-10 \text{ (meters, see SunQM-2's Table 2)} - 5.645E-15 \text{ (meters)} = 9.526E-10 \text{ meters.} \quad \text{eq-18}$$

$$r_{2,ap} = 2 * r_{2,circular} - r_{2,p} = 2 * 2.117E-10 \text{ (meters, see SunQM-2's Table 2)} - 5.645E-15 \text{ (meters)} = 4.234E-10 \text{ meters.}$$

eq-19

The $n=3$ (or $n=2$) electron has the same total orbital energy at the either perihelion site (see eq-1) or aphelion site. Thus,

$$E_{3,ap} = K + U = \frac{1}{2}mv_{n=3,gr,ap}^2 - \frac{Ze^2}{4\pi\epsilon_0 r_{3,ap}} = -2.421 \times 10^{-19} \text{ (Joule)} \quad \text{eq-20}$$

$$E_{2,ap} = K + U = \frac{1}{2}mv_{n=2,gr,ap}^2 - \frac{Ze^2}{4\pi\epsilon_0 r_{2,ap}} = -5.447 \times 10^{-19} \text{ (Joule)} \quad \text{eq-21}$$

Solving eq-20 (and eq-21), we have

$$v_{3,gr,ap} = 13195 \text{ m/s.} \quad \text{eq-22}$$

$$v_{2,gr,ap} = 19591 \text{ m/s.} \quad \text{eq-23}$$

and

$$\lambda_{3,ap} = h/(mv_{3,gr,ap}) = 6.626E-34 / (9.109E-31 * 13195) = 5.513E-8 \text{ meters,} \quad \text{eq-24}$$

$$\lambda_{2,ap} = h/(mv_{2,gr,ap}) = 6.626E-34 / (9.109E-31 * 19591) = 3.713E-8 \text{ meters.} \quad \text{eq-25}$$

So, an electron at $n=3$ elliptical orbit has a (large-sized) 3D wave packet (diameter $\approx 5.513E-8$ meters, orbital moving from aphelion to perihelion to aphelion at $|3,2,0\rangle$ orbit). During orbital transition, it spins-off its outmost shell to become a small-sized 3D wave packet (diameter $\approx 3.713E-8$ meters, orbital moving from aphelion to perihelion to aphelion at $|2,1,0\rangle$ orbit). However, (unlike that using the Bohr circular velocity can give both the orbital electron's 3D-wave packet size-shrinking and the emitted photon's 3D wave packet size), this calculation (using the transient velocity at the aphelion site) can only give the orbital electron's 3D-wave packet size-shrinking, it cannot give the emitted photon's 3D wave packet size. In contrast, the calculation using the transient velocity at the perihelion site does give the emitted photon's 3D wave packet size (it can be deduced from eq-17), but not the orbital electron's 3D-wave packet size-shrinking.

From this analysis, it confirmed that not only the size of a 3D wave packet of a photon is about one wavelength of the photon, but also the core of the 3D wave packet (of a photon) has a higher (wave) frequency (components) and it correlates to the electron movement at the perihelion site of the elliptical orbital transition, while the out-shells of the 3D wave packet (of a photon) has a lower (wave) frequency (components) and it correlates to the electron movement at the aphelion site of the elliptical orbital transition. Now let us re-explain this concept by using t_1 , t_3 , t_5 time points in electron orbit (in Figure 5b) and correlates them to the t_1 , t_3 , t_5 time points in photon's 3D wave packet (in Figure 7j):

- 1) At the t_1 time point, the electron is at the aphelion site of $|3,2,0\rangle$ elliptical orbit, and has the lowest orbital speed, and it starts to generate the wave-front of the 3D wave packet of the photon, so this wave-front (that correlated to the outmost shell of the 3D wave packet of the photon) has the lowest frequency (in the 3D wave packet of the photon);
- 2) At the t_3 time point, the electron is at the perihelion site of $|3,2,0\rangle$ elliptical orbit, and has the highest orbital speed, and it generates the core of the 3D wave packet of the photon, so that this core has the highest frequency (in the 3D wave packet of the photon);
- 3) At the t_5 time point, the electron is at the aphelion site of $|2,1,0\rangle$ elliptical orbit, and has the (second) lowest orbital speed (only a little bit higher than that at t_1), and it generates the wave-end of the 3D wave packet of the photon, so this wave-end (that correlated to the outmost shell of the 3D wave packet of the photon) has the (second) lowest frequency (in the 3D wave packet of the photon), and
- 4) it also caused the unsymmetrical 3D wave packet (because even both are at the outmost shell of the 3D wave packet, the wave-end has a little bit higher frequency than that of the wave-front).
- 5) Notice that the above explanation is based on the concept that the emitted photon is a 3D wave packet. Alternatively, we can re-explain the same process based on the concept that the electron is a 3D wave packet: the electron (at t_1 and) at the aphelion of $|3,2,0\rangle$ elliptical orbit (with the lowest orbital speed) forms the outmost shell of the electron's 3D wave packet (with the lowest frequency); the electron (at t_3 and) at the perihelion of $|3,2,0\rangle$ elliptical orbit (with the highest orbital speed) forms the core of the electron's 3D wave packet (with the highest frequency); the electron (at t_5 and) at the aphelion of $|2,1,0\rangle$ elliptical orbit (with the second lowest orbital speed) forms the second outmost shell of the electron's 3D wave packet (with the second lowest frequency), so the orbital transition from $|3,2,0\rangle$ to $|2,1,0\rangle$ at the perihelion site caused the electron's 3D wave packet spin-off its outmost shell (at the perihelion site), and its second outmost shell now becomes the new outmost shell.

II-k. A photon absorption process

For the explanation of a photon absorption process, if a photon has its 3D wave packet size at one wavelength, then a 656 nm photon has the size larger than Bohr H-atom's $r_{n=2}$ ($= 5.29E-11 * 2^2 = 2.12E-10$ meters ≈ 21 nm). So the whole H-atom is submerged in the photon while it absorbing the whole photon to make $n=2$ to $n=3$ transition. We still can explain this process as the opposite process of in Figure 5b (i.e., a photon from $-x$ to $+x$, hit a $|2,1,0\rangle$ orbital electron at the perihelion site, and pushed it to a more elongated $|3,2,0\rangle$ orbit). However, this explanation become a pure auxiliary explanation (because the probability is too low for a (light-speeded) photon to hit an (extreme high speed) electron at a very specific site (the perihelion site), so this process is not feasible). The true process of photon absorption may be through some kind of "orbital resonance" between $n=2$ and $n=3$ orbits (because $f_{2,ph} + \Delta f = f_{3,ph}$). On the other hand, the explanation of Figure 5b is also an auxiliary explanation (at beginning), but it may also describe a true physical process of how a photon is emitted (because this process is more feasible).

II-l. Summary and discussion (of section II):

Thus, in the " $|nL0\rangle$ elliptical orbital transition model", the 3D vector $\Delta\vec{p} \Delta\vec{x} \geq \hbar/2$ uncertainty is spread in the whole (one period of) elliptical orbit (started from aphelion, maximized at perihelion, then ended at aphelion), and it is not only at the perihelion position. However, we may (over) simplify it as $\Delta\vec{x} \equiv 0$, $\Delta\vec{p}$ only in θ -1D. Under this simplification, we can use the classical physics to calculate out that, for a $|3,2,0\rangle$ orbital moving electron (in xz -plane) at the perihelion position, it has a $r_{n=3,p}$ very close to the proton, it has the orbit speed close to the speed of light, and under the extreme sharp-turn, it spins-off the outmost shell (of 3D matter wave) as a photon, and this photon propagates in the tangential $+x$ direction (because it is neutral, not subject to the proton's attracting force). Meanwhile, the $|3,2,0\rangle$ orbital moving electron (in xz -plane) at the perihelion position suddenly (and quantumly) lost part of the orbital speed ($v_{n=3,p} - v_{n=2,p} \approx 1109$ m/s), so it falls into a less elongated elliptical orbital track (i.e., $|2,1,0\rangle$ track, still in xz -plane).

The $|3,2,0\rangle$ to $|2,1,0\rangle$ elliptical orbital transition description is more superior than the Bohr atom's $n=3$ to $n=2$ circular orbital transition description (in SunQM-6s1's Figure 1), because it gives the analysis of the force, the speed, the detailed direction, etc. We believe that both descriptions should be put into the "Feynman Pool" (see SunQM-7's Appendix G), because both are useful in describe the Bohr atom's $n=3$ to $n=2$ photon emission (although in different level of details).

The final goal of the whole design and development (on the H-atom's $n=3$ to $n=2$ orbital transition and photon emission) is, to use $\{N,n\}$ QM and NBP (non-Born probability) to fully (and simultaneously) describe:

- 1) the $|3,2,0\rangle$ elliptical orbit track (as explained in SunQM-7's Figure 3a);
- 2) the physical structure (or the 3D electromagnetic wave packet or 3D matter wave packet) of both electron and photon (see SunQM-6s1's Figure 3 and Figure 4); and
- 3) the electric and magnetic force field of H-atom (containing a proton and an electron).

We are few steps closer to this goal.

This " $|nL0\rangle$ elliptical orbital transition model" is not only applicable to the H-atom and the micro world, but also should applicable to the macro-world. We will show some examples in the next paper (SunQM-6s3).

III. Both "electron orbital track model" and " $|nL0\rangle$ elliptical orbital transition model" directly correlate to the NBP description

Originally, the “electron orbital track model” (in section I) is based on Born probability (which is the Schrodinger equation’s solution), and it is used to replace the electron cloud description. However, a true Born probability-based “electron orbital track model” needs to have two opposite directional orbital movements running on the same single track simultaneously (to form a standing wave), but in all above description (in sections I and II), we always only used one uni-directional orbital movement at a single time. So, more accurately, the “electron orbital track model” is correlate to the non-Born probability (NBP), rather than the Born probability. Similarly, the “ $|nL0\rangle$ elliptical orbital transition model” is also used to describe a uni-directional orbital movement at a single time, thus, it is also correlate to the NBP. Therefore, we (conceptually) unified the $|n/m\rangle$ QM state description with the $|n/m\rangle$ elliptical orbit description, and with the NBP description.

IV. Dis-entanglement of the outmost shell of a photon can happen in many processes, and may can be explained in many ways

Dis-entanglement of the outmost shell of a photon may can happen in many processes. For example, in Compton scattering (inelastic scattering), a (x-ray) photon partially absorbed by an orbital electron, and knock it out of an atom, and rest part of photon scattered away as a red-shifted photon. We can say that the out-shells of the photon is absorbed (by an electron), the core is scattered as the red-shifted photon. In theory, the scattered core of the photon (if it still has enough energy) can knock another electron out of another atom (by contributing its middle shells to the electron), and an even smaller core is scattered as the more red-shifted photon. So, for a single x-ray photon, this inelastic scattering can happen many times as long as the leftover core (of the photon) still has enough energy (to knockout the next orbital electron). This is a perfect example that a single photon can have its outmost multiple shells be stripped-off one after other, and thus be red-shifted again and again. The major difference is, Compton scattering (or one kind of inelastic scattering) is a random process, and the scattered (red-shifted) photon usually changed the original propagation direction (see wiki “tired light”), while the cosmic red-shift of an old-photon is a programmed process, and does not change photon’s original propagation direction.

Also, we probably may (or may not) use some other theories to explain the cosmic red-shift of an old photon. For example, in wiki “Group velocity”, “*Higher-order terms in dispersion ... If the wavepacket has a relatively large frequency spread, ... or if the packet travels over very long distances, ... higher-order terms in the Taylor expansion become important. As a result, the envelope of the wave packet not only moves, but also distorts, in a manner that can be described by the material's group velocity dispersion. Loosely speaking, different frequency-components of the wavepacket travel at different speeds, with the faster components moving towards the front of the wavepacket and the slower moving towards the back. Eventually, the wave packet gets stretched out*”. According to this theory, we may can draw the 3D wave packet of a photon in the following way: the (relatively high-frequency) core and inner-shells are moving faster than the (relatively low-frequency) middle-shells and out-shells, and the (relative lowest-frequency) outmost shell likes a (hanging) tail that can be dis-entangled easily (see Figure 9). (Note: In this case, not only the Δx of the photon’s 3D wave packet keeps growing, but the $\Delta p \Delta x$ also keeps increasing). (See SunQM-6s3’s Figure 8 for more discussion).

Giancoli’s text book (page 1115) mentioned that the violation of the energy conservation law in the early experiment of beta-decay made Wolfgang Pauli to propose the new particle “neutrino” (in 1930). Similarly, to solve the puzzle of the cosmic red-shift, we need to introduce a new (gigantic-sized) “particle”, i.e., the “low-f photon”, or the “sub-Hz photon” (instead of the expansion of universe). Again, all discussions (in this section) are trying to support the following hypothesis: it is the natural attribute of an old photon to produce the red-shift. It is just because the photon is too old, it is “decaying” (see the general “decay” theory of particle in SunQM-6s3’s Table 2). Nothing peculiar.

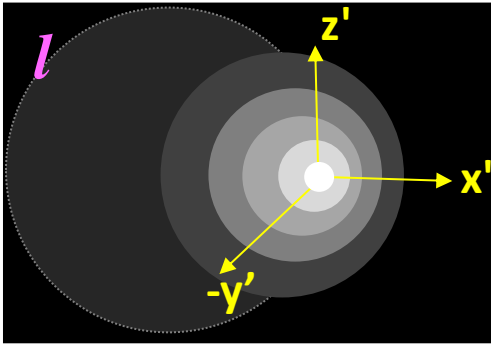


Figure 9. An alternative model of an old photon's 3D wave packet based-on wiki "Group velocity" that "*different frequency-components of the wavepacket travel at different speeds, ...*". Its (relatively high-frequency) core and inner-shells are propagating faster than the (relatively low-frequency) middle-shells and out-shells. Its (relatively lowest-frequency) outmost shell likes a tail that is usually being dragged around, and it will be detached (or dis-entangled) eventually (as an intrinsically programmed process).

Summary and Conclusion:

In section I, we first (roughly) unified the Schrodinger equation described electron movement in H-atom (i.e., the Born probability) to the $|n/m\rangle$ elliptical orbital motion described electron movement in H-atom. In section II, we (conceptually) unified all four different kind of wave explanations (1D-wave, 1D-wavepacket, 3D-wave, and 3D wave packet) for the photon emission and propagation. Then, by correlating all four different kind of wave explanations to the electron's elliptical orbital movement in H-atom, we successfully unified all four different kind of wave explanations to the orbital movement of the electron (for a photon's emission and propagation). The " $|nL0\rangle$ elliptical orbital transition model" makes us to believe strongly that the cosmic red-shift is one of the nature attributes of QM.

Acknowledgements:

Many thanks to: all the (related) experimental scientists who produced the (related) experimental data, all the (related) theoretical scientists who generated all kinds of theories (that become the foundation of $\{N,n/q\}$ QM theory), the (related) text book authors who wrote down all results into a systematic knowledge, the (related) popular science writers who simplified the complicated modern physics results into a easily understandable text, the (related) Wikipedia writers who presented the knowledge in a easily accessible way, the (related) online (video/animated) course writers/programmers who presented the abstract knowledge in an intuitive and visually understandable way. Also thanks to NASA and ESA for opening some basic scientific data to the public, so that citizen scientists (like me) can use it. Also thanks to the online preprinting serve vixra.org to let me post out my original SunQM series research articles.

Special thanks to: Fudan university, theoretical physics (class of 1978, and all teachers), it had made my quantum mechanics study (at the undergraduate level) become possible. Also thanks to Tsung-Dao Lee and Chen-Ning Yang, they made me to dream to be a physicist when I was eighteen. Also thanks to Shoucheng Zhang (张首晟, Physics Prof. in Stanford Univ., my classmate at Fudan Univ. in 1978) who had helped me to introduce the $\{N,n\}$ QM theory to the scientific community.

Also thanks to a group of citizen scientists for the interesting, encouraging, inspiring, and useful (online) discussions: "职老" (https://bbs.creaders.net/rainbow/bbsviewer.php?trd_id=1079728), "MingChen99"

(https://bbs.creaders.net/tea/bbsviewer.php?trd_id=1384562), “zhf” (https://bbs.creaders.net/tea/bbsviewer.php?trd_id=1319754), Yingtao Yang (https://bbs.creaders.net/education/bbsviewer.php?trd_id=1135143), “tda” (https://bbs.creaders.net/education/bbsviewer.php?trd_id=1157045), etc.

Also thanks to: Takahisa Okino (Correlation between Diffusion Equation and Schrödinger Equation. Journal of Modern Physics, 2013, 4, 612-615), Phil Scherrer (Prof. in Stanford University, who explained WSO data to me (in email, see SunQM-3s9)), Jing Chen (https://www.researchgate.net/publication/332351262_A_generalization_of_quantum_theory), etc. Note: if I missed anyone in the current acknowledgements, I will try to add them in the SunQM-9s1’s acknowledgements.

References

- [1] Yi Cao, SunQM-1: Quantum mechanics of the Solar system in a $\{N,n/6\}$ QM structure. <http://vixra.org/pdf/1805.0102v2.pdf> (original submitted on 2018-05-03)
- [2] Yi Cao, SunQM-1s1: The dynamics of the quantum collapse (and quantum expansion) of Solar QM $\{N,n\}$ structure. <http://vixra.org/pdf/1805.0117v1.pdf> (submitted on 2018-05-04)
- [3] Yi Cao, SunQM-1s2: Comparing to other star-planet systems, our Solar system has a nearly perfect $\{N,n/6\}$ QM structure. <http://vixra.org/pdf/1805.0118v1.pdf> (submitted on 2018-05-04)
- [4] Yi Cao, SunQM-1s3: Applying $\{N,n\}$ QM structure analysis to planets using exterior and interior $\{N,n\}$ QM. <http://vixra.org/pdf/1805.0123v1.pdf> (submitted on 2018-05-06)
- [5] Yi Cao, SunQM-2: Expanding QM from micro-world to macro-world: general Planck constant, H-C unit, H-quasi-constant, and the meaning of QM. <http://vixra.org/pdf/1805.0141v1.pdf> (submitted on 2018-05-07)
- [6] Yi Cao, SunQM-3: Solving Schrodinger equation for Solar quantum mechanics $\{N,n\}$ structure. <http://vixra.org/pdf/1805.0160v1.pdf> (submitted on 2018-05-06)
- [7] Yi Cao, SunQM-3s1: Using 1st order spin-perturbation to solve Schrodinger equation for nLL effect and pre-Sun ball’s disk-lyzation. <http://vixra.org/pdf/1805.0078v1.pdf> (submitted on 2018-05-02)
- [8] Yi Cao, SunQM-3s2: Using $\{N,n\}$ QM model to calculate out the snapshot pictures of a gradually disk-lyzing pre-Sun ball. <http://vixra.org/pdf/1804.0491v1.pdf> (submitted on 2018-04-30)
- [9] Yi Cao, SunQM-3s3: Using QM calculation to explain the atmosphere band pattern on Jupiter (and Earth, Saturn, Sun)’s surface. <http://vixra.org/pdf/1805.0040v1.pdf> (submitted on 2018-05-01)
- [10] Yi Cao, SunQM-3s6: Predict mass density r -distribution for Earth and other rocky planets based on $\{N,n\}$ QM probability distribution. <http://vixra.org/pdf/1808.0639v1.pdf> (submitted on 2018-08-29)
- [11] Yi Cao, SunQM-3s7: Predict mass density r -distribution for gas/ice planets, and the superposition of $\{N,n/q\}$ or $|qnlm\rangle$ QM states for planet/star. <http://vixra.org/pdf/1812.0302v2.pdf> (replaced on 2019-03-08)
- [12] Yi Cao, SunQM-3s8: Using $\{N,n\}$ QM to study Sun’s internal structure, convective zone formation, planetary differentiation and temperature r -distribution. <http://vixra.org/pdf/1808.0637v1.pdf> (submitted on 2018-08-29)
- [13] Yi Cao, SunQM-3s9: Using $\{N,n\}$ QM to explain the sunspot drift, the continental drift, and Sun’s and Earth’s magnetic dynamo. <http://vixra.org/pdf/1812.0318v2.pdf> (replaced on 2019-01-10)
- [14] Yi Cao, SunQM-3s4: Using $\{N,n\}$ QM structure and multiplier n' to analyze Saturn’s (and other planets’) ring structure. <http://vixra.org/pdf/1903.0211v1.pdf> (submitted on 2019-03-11)
- [15] Yi Cao, SunQM-3s10: Using $\{N,n\}$ QM’s Eigen n to constitute Asteroid/Kuiper belts, and Solar $\{N=1..4,n\}$ region’s mass density r -distribution and evolution. <http://vixra.org/pdf/1909.0267v1.pdf> (submitted on 2019-09-12)
- [16] Yi Cao, SunQM-3s11: Using $\{N,n\}$ QM’s probability density 3D map to build a complete Solar system with time-dependent orbital movement. <https://vixra.org/pdf/1912.0212v1.pdf> (original submitted on 2019-12-11)
- [17] Yi Cao, SunQM-4: Using full-QM deduction and $\{N,n\}$ QM’s non-Born probability density 3D map to build a complete Solar system with orbital movement. <https://vixra.org/pdf/2003.0556v2.pdf> (replaced on 2021-02-03)
- [18] Yi Cao, SunQM-4s1: Is Born probability merely a special case of (the more generalized) non-Born probability (NBP)? <https://vixra.org/pdf/2005.0093v1.pdf> (submitted on 2020-05-07)
- [19] Yi Cao, SunQM-4s2: Using $\{N,n\}$ QM and non-Born probability to analyze Earth atmosphere’s global pattern and the local weather. <https://vixra.org/pdf/2007.0007v1.pdf> (submitted on 2020-07-01)
- [20] Yi Cao, SunQM-5: Using the Interior $\{N,n/6\}$ QM to Describe an Atom’s Nucleus-Electron System, and to Scan from Sub-quark to Universe (Drafted in April 2018). <https://vixra.org/pdf/2107.0048v1.pdf> (submitted on 2021-07-06)
- [21] Yi Cao, SunQM-5s1: White Dwarf, Neutron Star, and Black Hole Explained by Using $\{N,n/6\}$ QM (Drafted in Apr. 2018). <https://vixra.org/pdf/2107.0084v1.pdf> (submitted on 2021-07-13)
- [22] Yi Cao, SunQM-5s2: Using $\{N,n/6\}$ QM to Explore Elementary Particles and the Possible Sub-quark Particles. <https://vixra.org/pdf/2107.0104v1.pdf> (submitted on 2021-07-18)
- [23] Yi Cao, SunQM-6: Magnetic force is the rotation-diffusion (RF) force of the electric force, Weak force is the RF-force of the Strong force, Dark Matter may be the RF-force of the gravity force, according to a newly designed $\{N,n\}$ QM field theory. <https://vixra.org/pdf/2010.0167v1.pdf> (replaced on 2020-12-17, submitted on 2020-10-21)
- [24] Yi Cao, SunQM-6s1: Using Bohr atom, $\{N,n\}$ QM field theory, and non-Born probability to describe a photon’s emission and propagation. <https://vixra.org/pdf/2102.0060v1.pdf> (submitted on 2021-02-11)
- [25] Yi Cao, SunQM-7: Using $\{N,n\}$ QM, Non-Born-Probability (NBP), and Simultaneous-Multi-Eigen-Description (SMED) to describe our universe. <https://vixra.org/pdf/2111.0086v1.pdf> (submitted on 2021-11-17)

- [26] David W. Kraft, "Relativistic Corrections to the Bohr Model of the Atom", American Journal of Physics 42, 837 (1974).
- [27] Stephen T. Thornton & Andrew Rex, Modern Physics for scientists and engineers, 3rd ed. 2006. p178 ~ p180.
- [28] Stephen T. Thornton & Andrew Rex, Modern Physics for scientists and engineers, 3rd ed. 2006. p180. "... the group velocity may be greater or less than the phase velocity. A medium is called nondispersive when the phase velocity is the same for all frequencies and $v_{gr} = v_{ph}$. An example is electromagnetic waves in vacuum".

Note: A series of my papers that to be published (together with current paper):

SunQM-4s4: More explanations on non-Born probability (NBP)'s positive precession in $\{N,n\}$ QM.

SunQM-6s3: Using Bohr atom, $\{N,n\}$ QM field theory, and non-Born probability to describe a photon's emission and propagation (part 3, drafted in June, 2022).

SunQM-6s4: Schrodinger equation and $\{N,n\}$ QM ... (drafted in January 2020).

SunQM-7s1: Relativity and non-linear $\{N,n\}$ QM

SunQM-9s1: Addendums, Updates and Q/A for SunQM series papers.

Note; Major QM books, data sources, software I used for SunQM series study:

Douglas C. Giancoli, Physics for Scientists & Engineers with Modern Physics, 4th ed. 2009.

David J. Griffiths, Introduction to Quantum Mechanics, 2nd ed., 2015.

John S. Townsend, A Modern Approach to Quantum Mechanics, 2nd ed., 2012.

Stephen T. Thornton & Andrew Rex, Modern Physics for Scientists and Engineers, 3rd ed. 2006.

James Binney & David Skinner, The Physics of Quantum Mechanics, 1st ed. 2014.

Wikipedia at: <https://en.wikipedia.org/wiki/>

(Free) online math calculation software: WolframAlpha (<https://www.wolframalpha.com/>)

(Free) online spherical 3D plot software: MathStudio (<http://mathstud.io/>)

(Free) offline math calculation software: R Microsoft Excel, Power Point, Word.

Public TV's space science related programs: PBS-NOVA, BBC-documentary, National Geographic-documentary, etc.

Journal: Scientific American.

Note: I am still looking for endorsers to post all my SunQM papers (including the future papers) to arXiv.org. Thank you in advance!

Appendix A. The whole set of $|3,l,m\rangle$ orbits can also be re-described as $|1,0,0\rangle$ orbit, and vice versa.

In some special cases, the whole set of $|3,l_{(=0..2)},m_{(=-l..+l)}\rangle$ orbits can also be re-described as $|1,0,0\rangle$ orbit that as shown in Figure 1d (if we set $n=3$ as the new $n'=1$), although the new span of $r_{n'=1}$ through $r_{n'=2}$ will be larger than the original span of $r_{n=3}$ through $r_{n=4}$. In other words, for an $n=3$ electron's $|3,l,m\rangle$ orbits, we still can force ourselves to use $n=1$, or $|1,0,0\rangle$ orbit to describe it. However, if we do so, we will mess-up all other n shells $\{N,n\}$ QM structure. Oppositely, the $|1,0,0\rangle$ orbit shown in Figure 1d can also be re-described as the whole set of $|n/m\rangle$ orbits at any n number (Note: it has to be $l=0..n-1$, and $m=-l..+l$). In other words, for an $n=1$ electron's $|1,0,0\rangle$ orbit, we still can force ourselves to use $n=3$, or $|3,l_{(=0..2)},m_{(=-2..+2)}\rangle$ orbits to describe it. Again, if we do so, we will mess-up all other $n(s)$ shells $\{N,n\}$ QM structure. Notice that the above n change is completely different from that in $\{N,n/q\}$ QM, where we can move r_1 inward (or outward) as we want (by using high-frequency n' , or sub-frequency n' , other than the base-frequency n), because using n' does not mess up the original QM structure.

For example, this is why in SunQM-4's explanation of eq-41 vs. eq-40, we can reset Earth's $\{1,5//6\}$ orbit, or $n=5$, or $n=5*6=30$, into $n'=1$. This is also why in SunQM-3s10's eq-40 deduction where we could choose $k = 2\pi/\lambda = 1$, or $\lambda = 2\pi$; or equivalent to in SunQM-4's eq-17, why we could choose $j=1$. Notice that this kind of unusual description will mess up the original QM description. For example, if we force Earth's $\{1,5//6\}$ orbit, or $n=5$, or $n=5*6=30$, into $n'=1$, we mess up the $\{N,n=2..6//6\}$ orbits for all the rest planets. The only advantage to do that is that we can simplify SunQM-4's eq-40 into SunQM-4's eq-41. On the other hand, the only way to change n without mess up the original $\{N,n/q\}$ QM structure is to change the original n into its high-frequency $n' = n * q^j$, where j is a positive integer (e.g., change Earth's $n=5$ to $5*6^1=30$, or $5*6^2=180$, etc.).

Usually, to force Figure 1d's $n=1$ to be a new $n'=3$, we get a new $|3,2,0\rangle$ orbital mode that it is not useful (because it messed up the original correct QM system). However, in some rare situations, it does help to explain something. For example, in the SunQM-5's Figure 3a and 3b, the protons of the elements (from $Z=11$ through $Z=118$) in the $\{-14,n=1..5//6\}$ super-shell was force to be in $n=2$, or $|2,l,m\rangle$ QM state, so that we can use the $|2,1,1\rangle$ and $|2,1,0\rangle$ QM states to explain the re-distribution of protons (among the nucleons) under the outside force-field in a more simplified way. Another example: in SunQM-4s2's Figure 3, to describe the $\{N,n\}$ QM structural origin for the subtropical and polar jet streams, the

Earth's atmosphere (that usually is described as $\{1,1//2\}$ QM state, or $n=1$, in Earth's $\{N,n//2\}$ QM structure), is now forced to be as $\{0,2//2\}$ QM state, or $n=2$ QM state, so that the subtropical and polar jet streams can be described as $|3,2,1\rangle$ and $|3,2,0\rangle$ QM states.

Appendix B. The rotation of an electric field line (but not the rotation of a charge) should be used to explain the direction of the magnetic field line

To make Figure 5's electron trajectory (t_1, t_2, t_3, t_4, t_5) to match to Figure 7d's \vec{B} vector orientation, we are forced to use the following concept, that is, it is the orbital rotation of a positive charge's electric field (straight) line \vec{E} vector that caused \vec{B} vector to show its vector direction. This concept correlates with the explanation of SunQM-6's Figure 5c perfectly: the self-spin of a positive charge rotates its electric field (straight) lines, and thus causes its \vec{B} field to change (from the original complete RF mode, i.e., no net \vec{B} vector showed-up) to the nL0 QM mode, i.e., a net \vec{B} field vector showed-up following the right-hand rule. In the case of H-atom (see Figure 5), the \vec{E} vector is formed from proton to electron, and the rotation of the \vec{E} is caused by the orbital moving of electron around the proton. This causes the net \vec{B} vector showed-up with the vector direction always points to the -y axis (based on the right-hand rule, if the electron orbital rotates anticlockwise in xz-plane as shown in Figure 5). A major deceleration of the motion electron near the perihelion region equals to add a strong clockwise orbital rotation of the \vec{E} vector, thus caused the net \vec{B} vector points to the +y direction (temporarily). This perfectly explained why the direction of \vec{B} vector is always oscillation in a photon's 1D transverse wave.

However, in SunQM-6's Figure 5a, a circular moving positive charge also produces a net \vec{B} vector in the same direction as that shown in SunQM-6's Figure 5c. If we try to use this saying, then, in Figure 5, the anticlockwise electron moving can be explained as the clockwise positive charge moving, the net \vec{B} vector normally points to +y direction, and the whole explanation will be messed up. So we should not use above saying. However, we can use this alternative saying: in a H-atom, both the proton and the electron are always face-to-face tidal-locked, and both are doing anti-clock orbital motion around their reduced mass center. Then the orbital moving of positive charge will produce a net \vec{B} vector points to the -y direction (according to SunQM-6's Figure 5a). Because the orbital radius (from the proton to the reduced mass center) is close to zero. This is equivalent to say, an anti-clock spinning \vec{E} vector (in xz-plane) will produce a \vec{B} vector pointing to -y direction.